Palaeogeography, Palaeoclimatology, Palaeoecology xxx (2010) xxx–xxx

Contents lists available at ScienceDirect

Palaeogeography, Palaeoclimatology, Palaeoecology

journal homepage: www.elsevier.com/locate/palaeo

Millennial-scale vegetation dynamics in an estuary at the onset of the Miocene Climate Optimum

Andrea Kern [a,*], Mathias Harzhauser [a], Oleg Mandic [a], Reinhard Roetzel [b], Stjepan Ćorić [b], Angela A. Bruch [c], Martin Zuschin [d]

[a] Natural History Museum Vienna, Geological-Paleontological Department, Burgring 7, 1010 Vienna, Austria
[b] Geological Survey of Austria, Neulinggasse 38, 1030 Vienna, Austria
[c] Senckenberg Research Institute and Natural Museum, Senckenberganlage 25, 60325 Frankfurt am Main, Germany
[d] University of Vienna, Department of Palaeontology, Althanstrasse 14, 1090 Vienna, Austria

ARTICLE INFO

Article history:
Received 13 January 2010
Received in revised form 14 July 2010
Accepted 16 July 2010
Available online xxxx

Keywords:
Pollen
Palaeoenvironment
Palaeoclimate
Late Burdigalian
Karpatian
Paratethys Sea

ABSTRACT

Pollen analyses have been proven to possess the possibility to decipher rapid vegetational and climate shifts in Neogene sedimentary records. Herein, a c. 21-kyr-long transgression–regression cycle from the Lower Austrian locality Stetten is analysed in detail to evaluate climatic benchmarks for the early phase of the Middle Miocene Climate Optimum and to estimate the pace of environmental change.

Based on the Coexistence Approach, a very clear signal of seasonality can be reconstructed. A warm and wet summer season with c. 204–236 mm precipitation during the wettest month was opposed by a rather dry winter season with precipitation of c. 9–24 mm during the driest month. The mean annual temperature ranged between 15.7 and 20.8 °C, with about 9.6–13.3 °C during the cold season and 24.7–27.9 °C during the warmest month. In contrast, today's climate of this area, with an annual temperature of 9.8 °C and 660 mm rainfall, is characterized by the winter season (mean temperature: −1.4 °C, mean precipitation: 39 mm) and a summer mean temperature of 19.9 °C (mean precipitation: 84 mm).

Different modes of environmental shifts shaped the composition of the vegetation. Within few millennia, marshes and salt marshes with abundant Cyperaceae rapidly graded into Taxodiaceae swamps. This quick but gradual process was interrupted by swift marine ingressions which took place on a decadal to centennial scale. The transgression is accompanied by blooms of dinoflagellates and of the green alga *Prasinophyta* and an increase in *Abies* and *Picea*. Afterwards, the retreat of the sea and the progradation of estuarine and wetland settings were a gradual progress again.

Despite a clear sedimentological cyclicity, which is related to the 21-kyr precessional forcing, the climate data show little variation. This missing pattern might be due to the buffering of the precessional-related climate signal by the subtropical vegetation. Another explanation could be the method-inherent broad range of climate-parameter estimates that could cover small scale climatic changes.

1. Introduction

Lower Miocene deposits of Austria are mainly represented by marine sediments of the Paratethys Sea, whereas well dated terrestrial strata are rare. An exception is the Korneuburg Basin in the north of Vienna (Fig. 1). This basin formed during the Burdigalian in the latest Early Miocene. The geology and palaeoecology of the Korneuburg Basin have been studied intensively within the last few years and presented in two monographs (Sovis and Schmid, 1998, 2002). During these studies a total of more than 650 taxa of fossil animals and plants have been described from this small basin. This enormous dataset allows a relatively detailed reconstruction of the palaeoenvironments (Harzhauser et al., 2002). Additional data on the palaeoecology were published by Zuschin et al. (2004) and Latal et al. (2005). According to these studies, the basin was strongly cut off from the open sea, where an estuary was formed in its southern part and more marine depositional environments prevailed in the north. There, the only small connection to the Paratethys was established. In the south, separated from the marine part by a tectonically induced swell, a broad array of coastal-terrestrial habitats became established, ranging from patches of an impoverished *Avicennia* mangrove via Taxodiaceae swamps to riparian forests (Hofmann et al., 2002). The coastal mudflats were inhabited by biostromes of the giant oyster *Crassostrea gryphoides*, which formed colonies of several thousands of individuals with shell sizes of up to 80 cm length. One of these biostromes was excavated during 2005–2008 by the Natural History Museum Vienna and is now part of the Geopark "Fossilienwelt Weinviertel". Contemporaneously, a major road construction project,

* Corresponding author. Fax: +43 1 52177 459.
E-mail address: andrea.kern@nhm-wien.ac.at (A. Kern).

0031-0182/$ – see front matter © 2010 Elsevier B.V. All rights reserved.
doi:10.1016/j.palaeo.2010.07.014

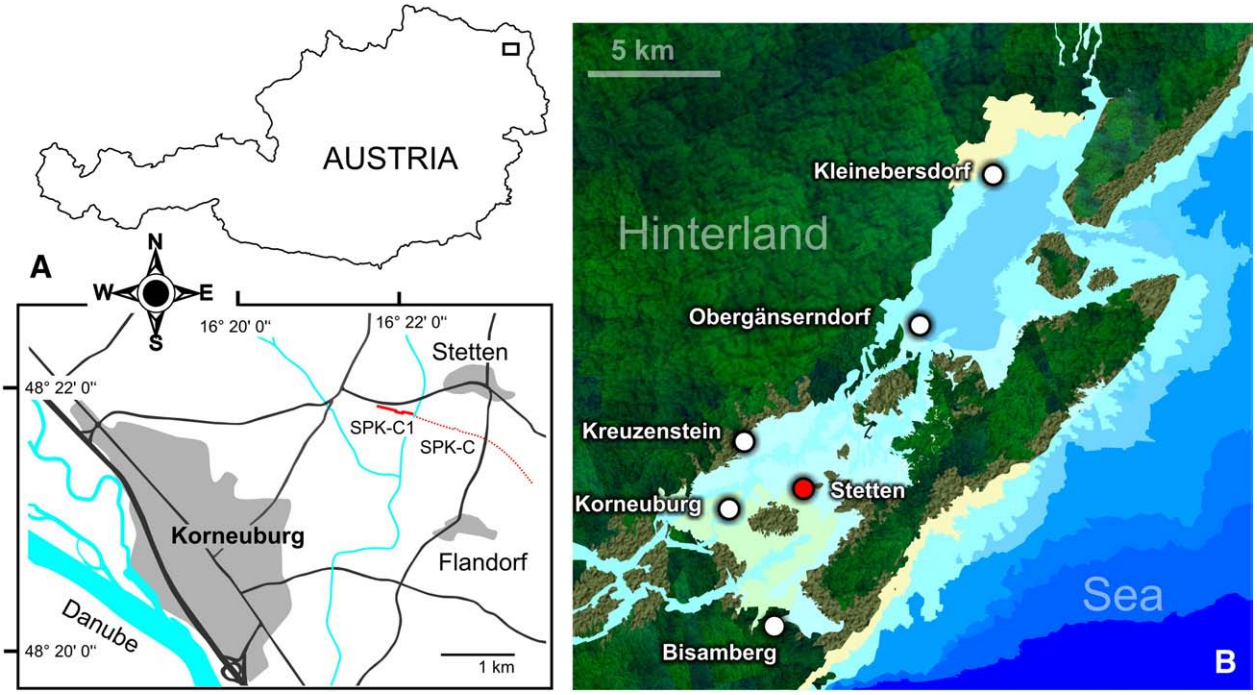

Fig. 1. A: geographic setting of the investigated section. The insert in the upper map indicates the position of the study area in north-eastern Austria. Full red line: SPK-C1, dotted red line: geologically documented section SPK. B: a strongly simplified paleogeographic reconstruction of the late Burdigalian Korneuburg Basin based on palaeoecological and sedimentological data (after Harzhauser et al., 2003, 2009). The red dot shows the position of the SPK-C1 section at the time of deposition. The sketch is an idealized illustration representing a phase when the Paratethys Sea reached far into the estuary corresponding more or less to the situation as represented by the samples SPK-C1 5 to 16. (For interpretation of the references to colour in this figure legend, the reader is referred to the web version of this article.)

the S1 motorway (Wiener Außenring-Schnellstraße) between the Tradenberg tunnel and the city of Korneuburg, was undertaken in the year 2008, allowing an exceptionally complete geological logging of a continuous section of the Miocene basin fill. The coincidence of both projects – providing palaeoecologic, stratigraphic and geologic backbones – gave rise to a sampling campaign on the palyno-assemblage studied in this paper.

Still, the mode of vegetational shifts in such Miocene estuaries is poorly studied, due to the usually very spotty preservation of accessible sediments. Moreover, as absolute datings and clear correlations with astronomical parameters are so far missing in the Lower Miocene deposits of central Europe, no estimation of the pace of the changes can be given. Herein, we try to quantify the observed vegetational shifts and to integrate the data in a hypothetic time/sedimentation rate model.

2. Geological setting

2.1. The Korneuburg Basin

The Korneuburg Basin (Fig. 1) is part of the Alpine-Carpathian thrust belt. It originated as a sub-basin of the Vienna Basin during its early stage. Reactivation of thrusts as strike-slip faults in the Lower Miocene caused a rapidly subsiding pull-apart type basin. The onset of the pull-apart phase of the Vienna Basin during the Middle Miocene, resulted in tilting of the Lower Miocene strata. The asymmetric SSW–NNE-oriented basin is c. 20 km long and attains a maximum width of 7 km, but is strongly narrowed in its northern extension. A central high separates the basin fill into two depocenters (Fig. 1B), the southern part with a sediment thickness of c. 880 m deep and a northern part of c. 530 m (Wessely, 1998). This swell was already active during the Early Miocene and caused a separation into a marine embayment in the north and an estuary in the south (Harzhauser et al., 2002). The basin margins are formed in the north by the Waschberg Unit and towards the south by the Rhenodanubian Flysch Unit. These Alpine-Carpathian nappes are underlain by the autochthonous basement formed mainly by Cretaceous and Jurassic units and by the crystalline of the Bohemian Massif. Sedimentation began during the Early Miocene (Eggenburgian) and comprised shallow marine marls and sands (Ritzendorf Formation). The main phase of deposition, however, started in the late Early Miocene (late Burdigalian = Karpatian in regional stratigraphy; Piller et al., 2007), represented by marly silts and fine to medium sands of the Korneuburg Formation. Rarely, gravel and boulder may occur in close position to the Flysch Zone; thin lignites of <1 m may occur as well.

According to palaeomagnetic measurements, a rather southern position of the area at c. 34° latitude was calculated by Scholger (1998) for the late Burdigalian Korneuburg Basin. Although this interpretation, requiring a northward movement of c. 1400 km since the late Burdigalian, seems to be an overestimation, a considerable northward shift is in accordance with other studies (Márton, 2008).

2.2. The SPK-C + SPK-C1 Stetten section

Due to c. 25° western tilting of the Karpatian deposits, during the Middle Miocene or later, the basin fill can be followed along a W–E transect. A c. 1.8 km long transect was geologically documented in detail in the southern part of the basin in the year 2008 (Fig. 1A). 324 sediment-samples, 118 molluscs-samples, 17 samples for diaspores and 118 palynosamples were taken for palaeontological, mineralogical and sedimentological analyses.

The c. 120-m-thick section comprises lignites, clay, silt, sand and rare pebble layers with abundant coquinas (Fig. 2A). The lower 30 m is characterized by pelitic sedimentation; its middle part between 30 and 75 m represents an intense alternation of pelites and psammites, whereas the top is dominated by sand. Internally, it may be divided into at least 6 coarsening–fining upward cycles. For this study, the lower 21 m of the section (N48°21′47.82″ E016°22′0.12″), representing one of these cycles was measured and sampled in more detail (Fig. 2B).

Please cite this article as: Kern, A., et al., Millennial-scale vegetation dynamics in an estuary at the onset of the Miocene Climate Optimum, Palaeogeography, Palaeoclimatology, Palaeoecology (2010), doi:10.1016/j.palaeo.2010.07.014

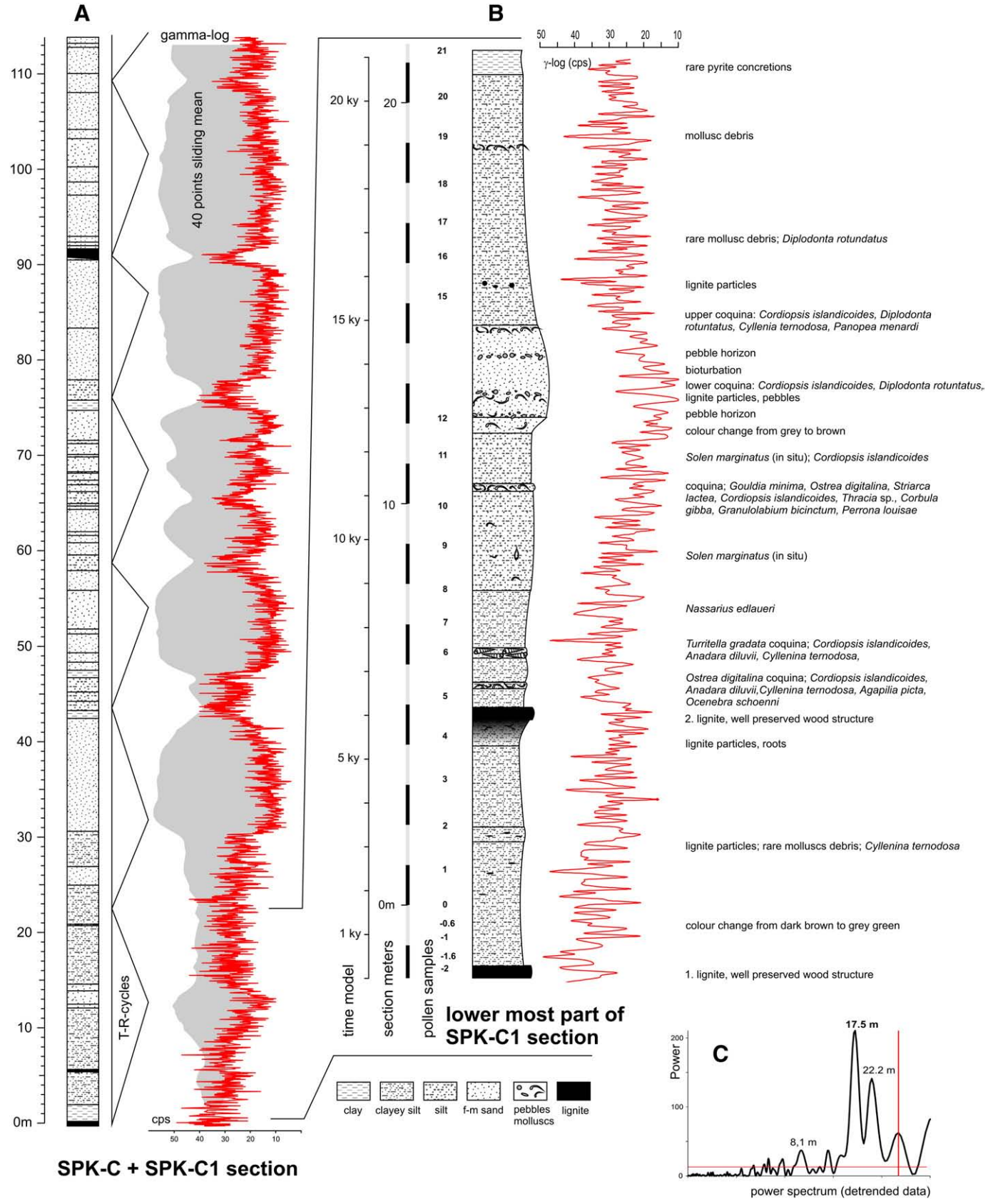

Fig. 2. Lithology of the SPK-C + SPK-C1 section (A) and detailed log of the lower part (B). A: the gamma-log and the sedimentary features reflect distinct coarsening–fining upward cycles which correspond to transgressive–regressive cycles (T–R-cycles). B: the lower part of the SPK-C1 section with typical mollusc assemblages and the position of the palynological samples. C: the spectral analysis performed on the gamma-log data, proves the existence of cycles which are interpreted as an expression of precessional forcing. Thus, the lowermost part of SPK-C1, spanning one of these cycles, might cover about 19–21 kyr.

Please cite this article as: Kern, A., et al., Millennial-scale vegetation dynamics in an estuary at the onset of the Miocene Climate Optimum, Palaeogeography, Palaeoclimatology, Palaeoecology (2010), doi:10.1016/j.palaeo.2010.07.014

Table 1
The table shows the counted results of all samples (SPK-C1 −2 to SPK-C1 21) for all determined pollen taxa. Additionally, percentage data of angiosperms opposed to gymnosperms and the percentages of gymnosperms, angiosperms, spores and dinoflagellates are shown.

	SPK-C1 −2	SPK-C1 −1.6	SPK-C1 −1	SPK-C1 −0.6	SPK-C1 0	SPK-C1 1	SPK-C1 2	SPK-C1 3	SPK-C1 4	SPK-C1 5	SPK-C1 6	SPK-C17
Percentages of determinded pollen taxa												
Pinus	9.09	11.32	32.00	5.56	14.93	14.71	29.17	0.00	0.00	7.59	5.47	5.64
Picea	4.55	0.00	4.57	4.17	2.99	5.88	8.33	6.25	0.00	1.90	3.48	5.02
Cathaya	2.27	11.32	18.86	8.33	9.70	20.59	20.83	6.25	20.00	4.43	5.97	9.09
Abies	2.27	0.00	4.00	0.00	0.75	2.94	0.00	6.25	0.00	1.27	2.49	5.33
Ephedra	0.00	0.00	0.00	0.00	0.00	2.94	0.00	0.00	0.00	0.00	0.00	0.31
Taxodiaceae	25.00	3.77	1.14	5.56	5.22	11.76	8.33	12.50	10.00	34.18	8.96	10.34
Sciadopitys	0.00	0.00	0.00	1.39	0.00	0.00	0.00	0.00	0.00	0.00	0.00	0.00
Carya	13.64	20.75	5.71	18.06	8.21	11.76	12.50	6.25	30.00	8.86	17.41	11.91
Pterocarya	4.55	16.98	6.86	16.67	12.69	8.82	0.00	0.00	10.00	2.53	7.96	9.40
Alnus	13.64	7.55	12.57	11.11	19.40	5.88	4.17	0.00	0.00	17.72	6.97	8.78
Engelhardia	2.27	5.66	1.14	1.39	2.24	0.00	0.00	6.25	10.00	6.96	12.94	7.52
Platycarya	0.00	0.00	0.00	1.39	1.49	0.00	0.00	0.00	0.00	2.53	1.00	4.70
Quercus	2.27	3.77	1.71	2.78	2.99	2.94	4.17	6.25	0.00	3.80	4.48	3.76
Celtis	4.55	0.00	0.57	1.39	0.00	0.00	0.00	6.25	0.00	0.00	0.00	0.31
Ulmus	2.27	1.89	0.00	4.17	1.49	2.94	0.00	0.00	0.00	1.90	1.49	1.57
Zelkova	0.00	1.89	0.00	0.00	0.00	0.00	0.00	0.00	0.00	0.63	0.50	0.31
Lonicera	0.00	0.00	1.14	0.00	0.75	0.00	0.00	0.00	0.00	0.63	1.99	0.63
Betula	0.00	0.00	0.00	1.39	0.75	0.00	0.00	0.00	0.00	0.00	0.00	0.00
Tiliaceae	0.00	0.00	6.86	6.94	5.97	2.94	0.00	0.00	0.00	0.63	1.00	0.31
Lythraceae	0.00	1.89	0.57	4.17	0.75	0.00	0.00	0.00	0.00	2.53	1.49	2.51
Oleaceae	0.00	1.89	0.57	0.00	0.00	0.00	0.00	0.00	0.00	0.00	3.48	1.57
Arecaceae	2.27	0.00	0.00	0.00	0.75	0.00	0.00	6.25	0.00	1.27	1.00	0.00
Symplocos	0.00	0.00	0.00	0.00	1.49	2.94	4.17	0.00	10.00	0.63	1.49	1.88
Poaceae	4.55	5.66	0.00	0.00	2.99	2.94	4.17	25.00	10.00	0.00	1.00	0.31
Fagus	0.00	0.00	0.00	0.00	0.00	0.00	0.00	0.00	0.00	0.00	0.00	0.31
Castanea	2.27	0.00	0.00	0.00	0.00	0.00	0.00	0.00	0.00	0.00	1.00	1.57
Carpinus	0.00	0.00	0.00	0.00	0.00	0.00	0.00	0.00	0.00	0.00	0.00	0.00
Liquidamber	0.00	1.89	0.00	0.00	0.75	0.00	0.00	0.00	0.00	0.00	0.50	0.00
Amaranthaceae	0.00	0.00	0.00	0.00	0.00	0.00	0.00	0.00	0.00	0.00	0.00	0.00
Chenopodiaceae	0.00	0.00	0.00	0.00	0.75	0.00	0.00	0.00	0.00	0.00	1.49	0.63
Artemisia	0.00	0.00	0.00	0.00	0.00	0.00	4.17	0.00	0.00	0.00	0.00	0.00
Mastrixoidae	0.00	0.00	0.00	0.00	0.00	0.00	0.00	0.00	0.00	0.00	0.00	0.00
Sapotaceae	0.00	0.00	0.00	0.00	0.00	0.00	0.00	0.00	0.00	0.00	0.00	1.57
Nyssa	0.00	0.00	0.00	0.00	0.75	0.00	0.00	0.00	0.00	0.00	0.00	0.00
Sparganium	0.00	0.00	1.14	2.78	0.00	0.00	0.00	0.00	0.00	0.00	0.00	0.31
Typha	0.00	0.00	0.00	0.00	0.00	0.00	0.00	0.00	0.00	0.00	0.00	0.00
Ilex	0.00	0.00	0.00	0.00	0.00	0.00	0.00	0.00	0.00	0.00	1.49	0.63
Myrica	0.00	1.89	0.00	0.00	0.00	0.00	0.00	0.00	0.00	0.00	0.00	0.00
Loranthaceae	0.00	1.89	0.00	1.39	0.75	0.00	0.00	0.00	0.00	0.00	0.50	0.00
Euphorbiaceae	0.00	0.00	0.00	0.00	0.00	0.00	0.00	0.00	0.00	0.00	0.00	0.31
Ericaceae	0.00	0.00	0.57	0.00	0.00	0.00	0.00	0.00	0.00	0.00	0.00	0.00
Rutaceae	0.00	0.00	0.00	0.00	0.00	0.00	0.00	6.25	0.00	0.00	0.50	0.94
Rubiaceae	0.00	0.00	0.00	0.00	0.00	0.00	0.00	0.00	0.00	0.00	0.00	0.94
Elegnaceae	0.00	0.00	0.00	0.00	0.00	0.00	0.00	0.00	0.00	0.00	0.00	0.00
Araliaceae	0.00	0.00	0.00	0.00	0.00	0.00	0.00	0.00	0.00	0.00	0.00	0.00
Vitaceae	0.00	0.00	0.00	0.00	0.00	0.00	0.00	0.00	0.00	0.00	0.00	0.00
Fagaceae	0.00	0.00	0.00	0.00	0.00	0.00	0.00	0.00	0.00	0.00	0.50	0.00
Apiaceae	0.00	0.00	0.00	0.00	0.00	0.00	0.00	0.00	0.00	0.00	0.00	0.00
Cyperaceae	0.00	0.00	0.00	0.00	0.00	0.00	0.00	6.25	0.00	0.00	0.00	0.00
Salix	0.00	0.00	0.00	1.39	0.75	0.00	0.00	0.00	0.00	0.00	1.49	0.00
Fraxinus	4.55	0.00	0.00	0.00	0.00	0.00	0.00	0.00	0.00	0.00	1.99	1.57
Asteraceae	0.00	0.00	0.00	0.00	0.75	0.00	0.00	0.00	0.00	0.00	0.00	0.00
Tricolporopollenites wackersdorfensis	0.00	0.00	0.00	0.00	0.00	0.00	0.00	0.00	0.00	0.00	0.00	0.00
Total pollen taxa	16	16	17	19	25	13	10	12	7	18	29	29
Percentages of												
Determined gymnosperms	43.18	43.18	26.42	26.42	60.57	25	33.58	58.82	66.67	31.25	30	49.37
Determined angiosperms	56.82	56.82	73.58	73.58	39.43	75	66.42	41.18	33.33	68.75	70	50.63
Percentages of spores, pollen, dinoflagellates and algae												
Gymnosperms	15.14	15.14	22.53	22.53	50.75	27.56	35.70	36.67	35.75	11.08	16.08	28.72
Angiosperms	42.16	42.16	51.10	51.10	30.45	49.33	46.45	35.56	31.84	45.12	29.37	54.05
Spores	41.62	41.62	23.63	23.63	16.92	15.11	16.99	24.44	26.26	42.22	21.68	16.89
Dinoflagellates	1.08	1.08	2.75	2.75	1.88	8.00	0.86	3.33	6.15	1.58	32.87	0.34
Green algae	0.00	0.00	0.00	0.00	0.00	0.00	0.00	0.00	0.00	0.00	0.00	0.00

It starts with c. 6 m clay and clayey silt with two prominent lignites of up to 50 cm thickness. Rootlets below the lignite indicate in-situ preservation. Above the lignite follows a 9-m-thick coarsening upward sequence of clay, clayey silt, silt, fine sand and medium sand (Fig. 2). An in-situ mass occurrence of the gastropod *Turritella gradata* occurs in the lower part. This coquina is a local marker bed

Please cite this article as: Kern, A., et al., Millennial-scale vegetation dynamics in an estuary at the onset of the Miocene Climate Optimum, Palaeogeography, Palaeoclimatology, Palaeoecology (2010), doi:10.1016/j.palaeo.2010.07.014

SPK-C1 8	SPK-C1 9	SPK-C1 10	SPK-C1 11	SPK-C1 12	SPK-C1 15	SPK-C1 16	SPK-C1 17	SPK-C1 18	SPK-C1 19	SPK-C1 20	SPK-C1 21
7.32	7.30	7.14	5.02	7.51	4.12	13.28	13.57	4.82	7.25	10.15	6.93
5.81	7.73	5.56	3.34	8.87	7.22	11.72	9.44	6.14	9.92	14.03	12.54
9.34	7.73	9.13	12.04	7.51	2.06	8.20	11.21	7.46	3.82	8.36	7.26
4.55	5.58	3.17	6.69	9.90	11.00	12.11	15.34	17.11	18.32	22.39	3.30
0.25	0.00	0.00	0.33	0.34	0.00	0.00	0.00	0.00	0.00	0.00	0.00
12.63	11.16	6.35	8.70	5.46	6.87	7.42	6.78	4.82	8.78	8.36	13.53
0.25	0.00	0.79	0.00	0.00	0.00	0.39	0.00	0.44	0.38	1.19	0.33
12.12	11.59	10.32	9.03	8.53	8.25	16.02	11.80	11.40	12.60	13.73	8.91
10.61	9.44	8.73	6.69	3.75	3.44	3.91	4.72	3.95	2.67	1.19	6.60
4.80	5.15	8.33	7.02	2.39	2.75	1.95	0.88	0.44	0.76	1.19	2.64
7.58	9.44	6.35	9.03	12.29	17.87	3.91	4.72	8.33	9.16	3.88	5.28
3.79	2.15	2.78	2.34	2.73	1.72	0.00	0.29	1.32	0.76	0.60	0.99
2.78	2.15	3.17	2.34	1.37	4.12	1.95	2.06	2.63	1.53	1.49	2.97
0.25	0.00	0.40	1.00	1.02	0.69	0.78	0.59	0.44	0.38	0.30	0.33
1.52	1.72	0.40	1.00	1.71	1.03	0.78	0.88	0.88	0.38	0.60	1.65
0.00	0.00	0.00	0.67	0.34	0.69	0.00	0.29	0.44	0.38	0.00	0.33
0.51	0.00	1.19	0.33	0.00	0.34	0.39	0.00	0.44	0.00	0.00	0.00
0.25	0.43	0.00	0.67	0.68	0.00	0.78	0.29	0.44	0.76	0.30	0.00
0.76	0.86	0.40	0.33	0.68	0.34	0.39	0.29	0.88	0.00	0.00	0.33
3.03	3.43	3.17	2.01	2.73	1.72	0.78	0.88	1.32	1.91	0.60	3.63
3.54	6.01	5.56	7.02	6.83	7.22	1.56	1.77	7.02	6.11	2.09	4.29
0.25	0.00	1.19	1.00	0.34	0.69	0.00	0.59	0.44	0.00	0.30	1.32
0.25	0.00	0.00	0.00	0.34	0.34	0.00	0.88	0.44	0.00	0.00	0.33
1.26	1.29	3.17	3.34	1.37	3.44	5.47	2.06	3.51	2.67	1.49	4.95
0.76	0.43	0.79	1.00	2.05	2.41	0.00	1.77	0.00	0.76	0.90	2.97
0.25	0.43	0.00	0.67	0.00	1.37	0.00	0.00	0.88	0.76	0.00	0.00
0.25	0.86	0.79	0.00	0.34	0.00	0.39	0.29	0.00	0.00	0.90	0.99
0.76	0.00	0.00	0.00	0.68	0.00	0.78	0.00	0.44	0.38	0.00	0.00
0.25	0.00	0.00	0.00	0.00	0.00	0.00	0.00	0.88	0.00	0.00	0.00
0.00	0.43	1.59	2.01	3.75	3.44	0.78	1.77	4.39	2.67	1.79	0.33
0.00	0.00	0.40	0.00	0.68	0.34	0.00	0.00	0.00	0.00	0.00	0.00
0.51	0.86	0.00	0.00	0.34	0.34	1.17	0.29	0.00	0.00	0.60	0.00
0.51	0.00	0.40	0.00	0.00	0.00	0.00	0.00	0.00	0.38	0.00	0.00
0.00	0.00	0.40	1.67	1.02	1.03	0.00	0.00	0.00	0.76	0.00	0.00
2.02	1.29	4.76	0.33	0.00	1.72	1.17	2.06	3.07	1.53	1.49	3.63
0.00	0.00	0.00	1.67	1.71	0.34	1.17	0.88	1.75	0.76	1.19	0.66
0.00	0.00	0.00	0.33	0.00	0.00	0.39	0.00	0.44	0.00	0.00	0.33
0.00	0.00	0.00	0.00	0.00	0.00	0.00	0.00	0.00	0.00	0.00	0.00
0.00	0.00	0.00	0.00	0.00	0.00	0.00	0.29	0.00	0.00	0.00	0.00
0.00	0.00	0.00	0.00	0.00	0.00	0.00	0.00	0.00	0.00	0.00	0.33
0.00	1.72	0.00	0.00	0.34	0.69	0.00	0.00	0.00	0.38	0.00	0.00
0.00	0.43	0.79	0.33	0.34	0.69	0.78	0.00	0.00	0.38	0.00	0.00
0.00	0.00	0.00	0.00	0.00	0.00	0.00	0.00	0.00	0.00	0.00	0.00
0.00	0.00	0.00	0.00	0.00	0.69	0.00	0.29	0.00	0.00	0.00	0.00
0.00	0.00	0.00	0.00	0.00	0.00	0.00	0.29	0.00	0.00	0.00	0.66
0.00	0.00	0.00	0.00	0.00	0.00	0.00	0.29	0.00	0.00	0.00	0.00
0.00	0.00	0.00	0.00	0.00	0.00	0.00	0.00	0.00	0.00	0.00	0.00
0.00	0.00	0.00	0.00	0.00	0.00	0.00	0.00	0.00	0.00	0.30	0.00
0.00	0.00	0.00	0.00	0.00	0.00	0.00	0.29	0.00	0.76	0.00	0.00
0.25	0.00	0.40	0.67	0.00	0.00	0.78	1.77	1.32	1.15	0.60	0.33
1.01	0.43	2.38	1.34	1.71	1.03	0.78	0.29	1.75	0.76	0.00	0.00
0.00	0.00	0.00	0.00	0.00	0.00	0.00	0.00	0.00	0.00	0.00	0.00
0.00	0.00	0.00	0.00	0.34	0.00	0.00	0.00	0.00	0.00	0.00	1.32
33	25	30	32	34	33	29	34	32	31	27	31
26.37	35.74	40.15	39.48	32.14	31.27	53.13	56.34	40.79	48.47	64.48	43.89
73.63	64.26	59.85	60.52	67.86	68.73	46.88	43.66	59.21	51.53	35.52	56.11
25.14	40.61	32.74	30.39	21.23	15.23	31.42	30.10	26.07	22.58	33.63	27.65
50.47	37.33	50.53	49.41	48.11	26.40	18.93	22.62	27.94	25.49	17.22	39.23
18.95	8.60	8.30	10.87	12.74	2.88	2.92	4.00	3.21	5.59	4.73	7.97
5.44	5.09	5.10	8.49	13.21	25.05	45.02	40.99	33.82	34.46	41.71	22.54
0.00	8.37	3.32	0.85	4.72	30.45	1.71	2.30	8.96	11.87	2.69	2.62

and can be traced, without change of density and structure, throughout the construction area. The silty middle part bears in-situ occurrences of the razor clam *Solen marginatus* along with scattered mollusc debris. This pattern changes completely in the 2-m-thick sandy unit which bears 2 prominent tempestitic coquinas consisting mainly of disarticulated bivalves. Two thin pebble lags accompany the

Please cite this article as: Kern, A., et al., Millennial-scale vegetation dynamics in an estuary at the onset of the Miocene Climate Optimum, Palaeogeography, Palaeoclimatology, Palaeoecology (2010), doi:10.1016/j.palaeo.2010.07.014

coquinas. The top part is represented by a fining upward sequence of silt and clay with scattered plant debris and rare coquinas.

2.3. Dating and time/sedimentation rate model

The Karpatian deposits are of latest Early Miocene age. The correlation of the mammal fauna with palaeomagnetic data allowed a dating into the early mammal zone MN 5, spanning a time of about 16.5–16.7 Ma (Daxner-Höck, 1998; Harzhauser et al., 2002). Due to the co-occurrence of calcareous nannoplankton zonal markers *Helicosphaera ampliaperta* Bramlette and Wilcoxon, 1967 and *Sphenolithus heteromorphus* Deflandre, 1953 the investigated samples can be placed into Zone NN4 (Martini, 1971). Early Miocene nannofossil assemblages contain *Coccolithus pelagicus* (Wallich, 1871) Schiller, 1930, *Cyclicargolithus floridanus* (Roth and Hay, 1967) Bukry, 1971, *Helicosphaera carteri* (Wallich, 1877) Kamptner, 1954, *Reticulofenestra excavata* Lehotayová, 1975, *Reticulofenestra gelida* (Geitzenauer, 1972) Backman, 1978, *Reticulofenestra pseudoumbilica* (Gartner, 1967) Gartner, 1969, and high percentages of reworked Cretaceous and Paleogene taxa. See Piller et al. (2007) for the correlation of the regional stages of the Paratethys realm with the standard stages.

The complete 1.8 km long section has been measured by a hand-held gamma-radiometer to evaluate the character and interpret the cause of cyclic changes observed during sedimentological logging. The final dataset grew to more than 17,000 measurements, all with fixed stratigraphic positions in the lithological column. Throughout the succession, the spectral analysis of the gamma-log data detected prominent, highly significant periodicities with a stratigraphic distance ranging from 17.5 m to 22.5 m (Fig. 2C). Lithologically, these periodicities are also well expressed by coarsening–fining upward rhythms, culminating in shore-sand units separated by clay or sandy clay (Fig. 2A). A detailed analysis of the total succession will be given elsewhere; for this study, however, the detailed palynological analysis of the lower 21 m of the section is discussed. The working hypothesis is that the observed cycles are either pure autocycles triggered by subsidence or that they are expressions of the 21-kyr-precession signal — or a combination of both. An interpretation of the sedimentary cycles as expression of the 100-kyr-eccentricity signal is ruled out as it would result in a 2-myr-long phase of sedimentation. This, however, is far too long for the late Karpatian with a duration of less than 1 ma (Piller et al., 2007).

Considering the cycles as the 21-kyr-precession signal would result in an average sedimentation rate of roughly 0.8–1.1 mm per year. This sedimentation rate fits well to the basin type with rapid subsidence and is therefore somewhat higher than in the later pull-apart phase of the Vienna Basin, when sedimentation rates between 0.4 and 0.6 mm per year are typical (Hohenegger et al., 2008; Lirer et al., 2009). Although the proposed Miocene sedimentation rates in the Korneuburg Basin are higher than in the neighbouring Vienna Basin, they are comparable with modern values in estuarine and lagoonal settings. Tropical to subtropical estuaries with rates of 1–10 mm/yr are documented from Western Africa (Debenay et al., 1994), Brazil (Patchineelam and Smoak, 1999; Behling et al., 2001) and South East Asia (Li et al., 2006; Ellison, 2005). Comparably high values of 0.5–1.8 mm/yr are also known from the precolonial Chesapeake Bay (Donoghue, 1989). Such high sedimentation rates are especially well documented from tropical mangals, ranging from 1.2 to 2.4 mm/yr (Lynch et al., 1989; Smoak and Patchineelam, 1999; van Santen et al., 2007) up to c. 11 mm/yr (Kamaruzzaman and Ong, 2008). Moreover, high sedimentation rates were supported by synsedimentary tectonic activity generating a depocenter in the Korneuburg Basin. Increasing relief energy in the Alpine hinterland and the North Alpine Foreland Basin caused high sediment supply to fill the newly generated accommodation space (Wessely, 1998).

Thus, the investigated cycle should reveal patterns related to autocyclic mechanisms or astronomic forcing spanning roughly 21,000 years, which may represent one full precession cycle. The sample density (one sample each meter) should thus account for a time resolution of c. 800–1000 years per sample.

3. Material and methods

The samples were taken during the highway construction close to Stetten in Lower Austria. For this investigation, 24 palynosamples were processed to evaluate preservation, diversity and composition of the palynomorph assemblages. Except for the sand unit at m 12–14 (Fig. 2B), where preservation is too poor for analysis, all samples were derived from clay and silt parts.

The samples were processed with hydrochloric acid (HCl conc.) and HF (hydrofluoric acid conc.) to eliminate all silica and calcareous matter. Afterwards the preparation followed the procedure of Klaus (1987) using glacial acidic acid (CH_3COOH conc.) before acetolysis was performed (Erdtman, 1954). Finally, after washing and sieving the samples with a 6 μm nylon sieve, the material was transferred into a glass tube and kept in glycerin. Between samples SPK-C1 −2 and 4 at least 150 pollen were counted due to bad preservation, for the rest an amount of more than 200 was identified (excluding *Pinus*). All samples are stored in the collection of the Natural History Museum Vienna (NHMW Inv. 2009B0004/001–2009B0004/064).

The software “Past” was used for cluster analyses and non-metric Multidimensional Scaling (nMDS) (Hammer et al., 2001). The pollen diagram was created by Tilia and Tilia-Graph (Grimm, 2004).

Climatic reconstructions were based on the counted pollen data, which were analysed by using the Coexistence Approach (Mosbrugger and Utescher, 1997). For the calculation of the climatic intervals, climatic data of the most appropriate nearest living relative of each taxon were considered. Taxa, which are today only limited to a much retreated area, such as *Cathaya* or *Sciadopitys*, were excluded from the analysis, because their recent distribution might not reflect their Miocene habitat requirements. Also, if they were limiting an interval, the Pinaceae pollen and the rare taxon *Ephedra* were not considered. Because of the ability of their pollen to spread over long distances their presumable living environment may have been far away.

For the remaining taxa, the natural worldwide distribution was considered to reflect the interval of their possible climatic viability. Taking all taxa into account, a climatic interval can be deduced, in which all these taxa can survive and “co-exist”. This is called the coexistence interval and is presented here as the climatic interval, in which the fossil taxa are most likely to have existed.

4. Results

In total, 24 samples were investigated; all samples contain pollen, spores and dinoflagellate cysts (Table 1; Figs. 3 and 4). In addition, spores of fungi, chitinous inner tests of foraminifera and lignite particles are abundant. High amounts of pyrite characterize all samples.

Samples from the lower most part of the section (SPK-C1 −2 to 4), situated between the prominent lignites, are poorly preserved. Here the assemblages are low diverse as a result of taphonomic bias (only thick-walled pollen and spores are preserved). Starting with sample SPK-C1 6, the number of taxa increases and the preservation improves. All samples contain small fragments of lignite, which are most abundant between the two lignite layers (SPK-C1 −2 to 5).

In most samples (SPK-C1 4–16, 18, 21) angiosperms are more abundant than gymnosperms. The angiosperms *Carya*, *Engelhardia*, *Pterocarya*, *Alnus*, *Quercus*, *Sparganium*, Oleaceae, Lythraceae and Poaceae attain percentages over 10%. Tiliaceae, Chenopodiaceae, *Fagus*, Symplocaceae, *Ulmus*, *Fraxinus* and *Salix* appear with more than 5%. Among the gymnosperms no family is clearly dominant unlike among the angiosperms, where *Carya*, *Pterocarya* and *Engelhardia* are the most abundant elements.

Please cite this article as: Kern, A., et al., Millennial-scale vegetation dynamics in an estuary at the onset of the Miocene Climate Optimum, Palaeogeography, Palaeoclimatology, Palaeoecology (2010), doi:10.1016/j.palaeo.2010.07.014

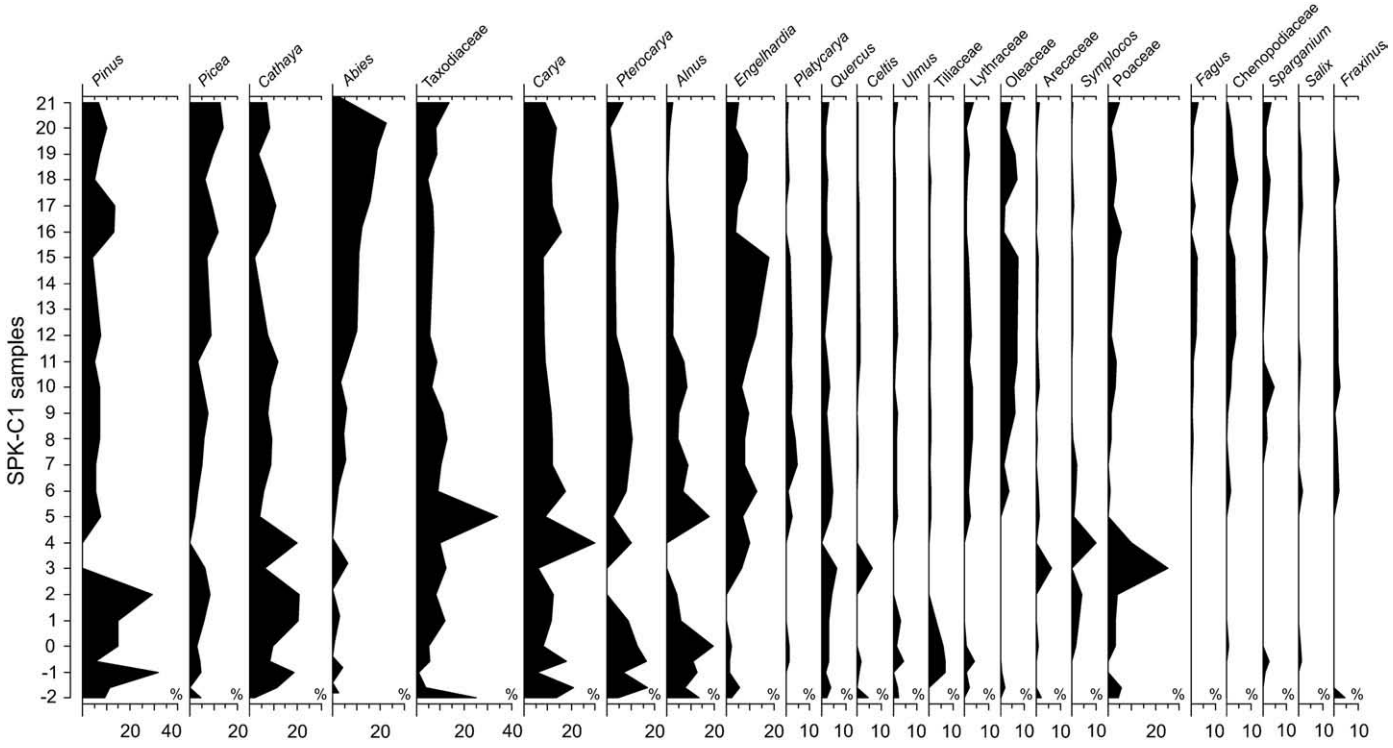

Fig. 3. Pollen diagrams reduced to the most significant angiosperms and gymnosperms.

A cluster analysis (Ward's method and paired group) of the data set (excluding undetermined counts, undetermined Pinaceae and extremely rare elements) revealed several distinct and robust groupings (Fig. 5A). Cluster I unites samples from the lowermost part of the section (SPK-C1 −2 to 4). These samples are rich in *Carya*, *Cathaya*, *Pinus*, *Pterocarya*, *Alnus*, Pteridaceae, Schizaeaceae and Tiliaceae. Cluster II encompasses samples SPK-C1 6–11. This cluster is characterized by coincident high abundances of *Carya*, *Cathaya*, *Engelhardia*, Taxodiaceae, *Pterocarya*, *Platycarya* and *Alnus* accompanied by Oleaceae, *Sparganium*, *Quercus*, *Lonicera* and Lythraceae. No group dominates the spectra. Cluster III is formed by samples SPK-C1 12 to 20. Although, *Carya*, *Engelhardia*, *Cathaya* and Taxodiaceae are still well represented, the increase of *Abies* and *Picea* is characteristic. Additionally Chenopodiaceae, *Sparganium*, Poaceae and Oleaceae are important constituents of the samples. In contrast, *Alnus*, *Symplocos*, *Platycarya*, Rutaceae and Arecaceae become rare elements. Within this main cluster, a subcluster (samples SPK-C1 16, 17, 20) forms which is characterized by comparably lower levels of *Engelhardia* and Oleaceae but increased occurrences of *Pinus* and *Cathaya*. This interval is also characterized by a distinct increase of dinoflagellates and a decrease of spores (Fig. 4). Above sample SPK-C1 12, the dinoflagellates are the dominating group of the playno-assemblage with up to 63.5%. Along with the dinoflagellates, the green algae *Prasinophyta* appears with a prominent peak in SPK-C1 15. It starts in low numbers in SPK-C1 7, and rises significantly in samples SPK-C1 12 and 15, thus spanning the barren sandy interval. Sample SPK-C1 5 forms the cluster IV; it is an outlier in all cluster analyses and also in nMDS plots (Fig. 5B), caused by abundance peaks of Taxodiaceae, *Glyptostrobus* and *Alnus*.

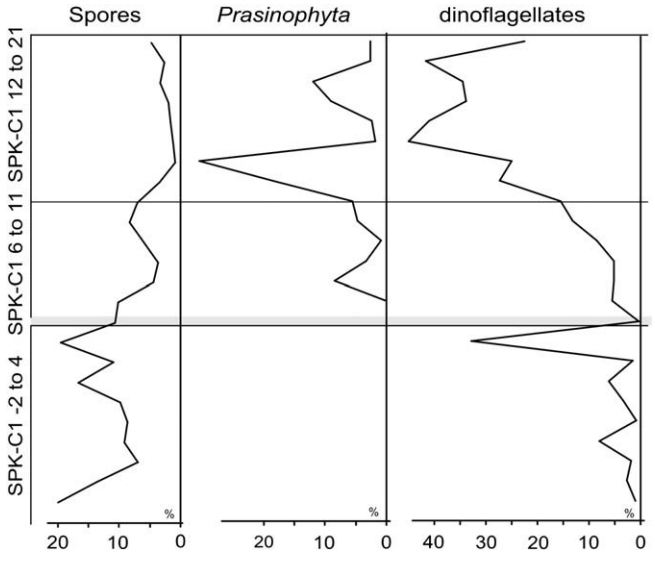

Fig. 4. Frequencies of spores, *Prasinophyta* and dinoflagelltes in the samples in percent. Spores and dinoflagellates display an opposing trend. The green flagellate *Prasinophyta* has a remarkable peak in the upper part of the section close to the foreshore and shoreface interval.

Finally, several samples tend to form poorly supported clusters or, depending on method, group differently. These are especially those samples with poor preservation and low numbers of counts. Only SPK-C1 21 is an exception. Although generally close to samples of cluster III, it differs by a distinct drop of *Abies* and a slight increase in Taxodiaceae. The nMDS plot reveals a similar pattern (Fig. 5B). The outliers SPK-C1 5 and SPK-C1 −1.6 are both lignite-related samples. Clusters I, II and III group within distinct regions and tend to be arranged along a stratigraphic axis. The clusters are also robust in a cluster analysis based on percentages of taxa (Fig. 6), which are also clearly dominant in different parts of the section (Fig. 7). Now the uniting elements of cluster I are *Cathaya*, *Pinus*, *Pterocarya*, *Carya* and *Alnus. Engelhardia*, *Abies* and *Picea* group within cluster III. Taxodiaceae still represent a maverick position corresponding to cluster IV. Thus, despite the supposed short time interval represented by the samples, statistically robust quantitative and qualitative differences of the palyno-assemblages suggest major shifts in ecological parameters.

Please cite this article as: Kern, A., et al., Millennial-scale vegetation dynamics in an estuary at the onset of the Miocene Climate Optimum, Palaeogeography, Palaeoclimatology, Palaeoecology (2010), doi:10.1016/j.palaeo.2010.07.014

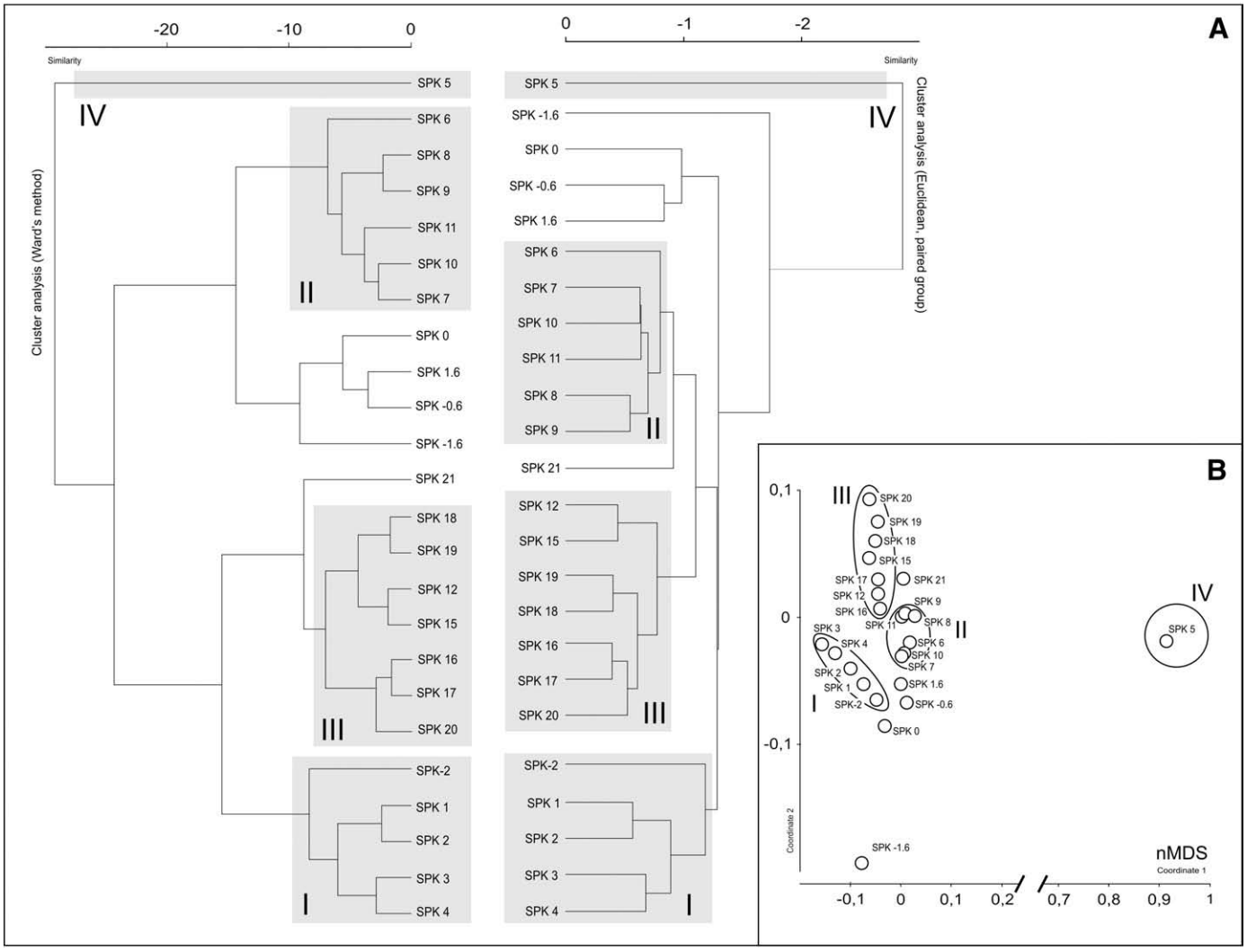

Fig. 5. A: Q-mode cluster analyses of the data (left: Ward's method, right: paired group) revealing several robust groupings of samples, which are also evident in the nMDS plot (B); see text for discussion. SPK −2 to 21 samples in the cluster refer to SPK-C1 −2 to 21.

5. Discussion

5.1. Palaeoenvironments

The southern part of the Korneuburg Basin was interpreted by Harzhauser et al. (2002) and Latal et al. (2005) as an estuary (Fig. 1B). A high number of biota were reconstructed ranging from shallow sublittoral shore face settings, mudflat coasts, *Crassostrea* biostromes, *Avicennia* thickets, coastal Taxodiaceae swamps, riparian forests to mixed-mesophytic forests in the hinterland. For the investigated part of the SPK-C1 section an interpretation of the depositional environments can be performed on the autochthonous invertebrate faunas and sedimentary features. This may serve as base for further interpretations of the par-autochthonous or allochthonous palyno-assemblages.

5.1.1. Autochthonous brackish-marine depositional environments

The lower part of the section, covered by the samples SPK-C1 −2 to 4, bears rare brackish-marine molluscs such as the nassariid gastropod *Cyllenina ternodosa*. These are usually confined to extremely shallow sublittoral to intertidal mud flat environments (Zuschin et al., 2004). The decrease of mollusc hash towards the lignite at 4.4–4.8 m and the low diversity of the mollusc assemblage indicate a gradual shift towards brackish or freshwater conditions which peak in the formation of a Taxodiaceae swamp. In correlative parts of the section, the occurrence of unidentifiable planorbid gastropods supports the interpretation of a freshwater swamp.

Marine conditions became re-established soon after. Above sample SPK-C1 5, a thin *Ostrea digitalina* coquina with neritid, nassariid and muricid gastropods (*Agapilia pachii*, *Cyllenina ternodosa*, *Ocenebra schoenni*) and disarticulated bivalves such as *Cordiopsis islandicoides* and *Anadara diluvii* formed at 5.4 m. Throughout the Late Oligocene and Early Miocene, such assemblages are highly indicative for estuaries and brackish lagoons (Baldi, 1973; Harzhauser and Mandic, 2002; Mandic et al., 2004). At 6.2 m, a second coquina appears, consisting mainly of *Turritella gradata*, a large sized turritellid gastropod. The shells are more or less in life-position and lack any post-mortem orientation by currents. Articulated valves of the venerid *Cordiopsis islandicoides* are additional indicators for such calm conditions. Elements of the asteroid starfish *Luidia?* sp. point to a strong marine influence in the estuary at that time. Starfishes like *Luidia* prefer normal marine conditions and only rarely tolerate salinities of less than 20 ppt (Hendler et al., 1995). Therefore, this part of the section is interpreted as a calm, soft-bottom lagoonal environment which initially was settled by *Ostrea digitalina* colonies in littoral settings which soon became replaced by subtidal environments with huge *Turritella* populations. The section interval between 8 and 11.8 m is characterized by a coarsening upward trend and a

Please cite this article as: Kern, A., et al., Millennial-scale vegetation dynamics in an estuary at the onset of the Miocene Climate Optimum, Palaeogeography, Palaeoclimatology, Palaeoecology (2010), doi:10.1016/j.palaeo.2010.07.014

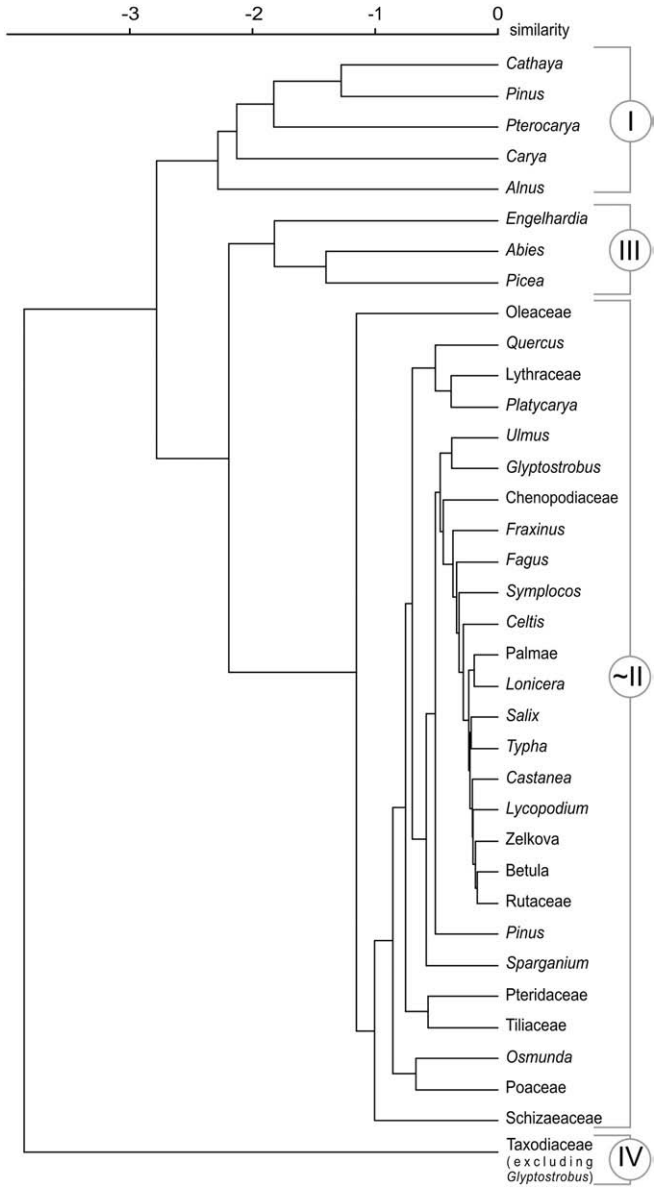

Fig. 6. A percentage-based R-mode cluster analysis of the data set was performed to test which taxa unite sample-groupings defined in Fig. 5.

change in the mollusc fauna. Intertidal elements such as *Nassarius edlaueri* are replaced by the large razor clam *Solen marginatus*, typical for shoreface environments (Mandic et al., 2008). The solenoids are found in life-position in the silty and sandy sediment. A first tempestite was formed at 10.4 m, pointing to a gradual increase of water energy. The mollusc assemblage with *Ostrea digitalina*, *Striarca lactea*, *Gouldia minima*, *Cordiopsis islandicoides*, *Thracia* sp., *Corbula gibba*, *Granulolabium bicinctum* and *Perrona louisae* represents a mixture of intertidal and sublittoral elements and reflects the proximity of mudflats and sandy foreshore settings.

This trend culminates in the sandy unit between 11.8 m and 14.4 m. Tempestites, shell and pebble lags indicate high wave energy in foreshore and shore settings. A color change from green–blue–grey towards ochre–yellow suggests an increased aeration of the sediment by repeated reworking by waves and by intense bioturbation. This is documented by poorly preserved, rare *Ophiomorpha–Thalassinoides*-like traces. The estuarine–marine character of the assemblages is obvious from elements such as the ungulinid *Diplodonta rotundata* and the geoduck *Panopea menardi*. The latter genus forms large populations in the subtidal zone and is extremely deep burrowing, attaining depths of more than 1 m (Gribben et al., 2004). The absence of deeply burrowed in-situ shells and the occurrence of disarticulated shells in the coquina may thus point to heavy wavy agitation leading to considerable reworking of the sediments. Upsection, the water energy decreases distinctly. Silty clayey sediments prevail; molluscs are represented by rare shells of *Diplodonta rotundata* and shell fragments. Even mudflat species are missing. A single thin coquina consisting of unidentifiable shell hash formed at 19.0 m. The low diversity and the predominance of a single species point to restricted environmental conditions which did not allow the establishment of marine taxa. Moreover, a poor oxygenation of the bottom is indicated by the increase of pyrite. This development points to a late phase of the marine ingression, heralding the progradation of lagoonal environments and the end of this sedimentary cycle.

5.1.2. Terrestrial environments

The cluster analysis already documented considerable vegetation shifts within the sedimentary cycle. The lowermost section (SPK-C1 −2 to 4; cluster I), is characterized by a low pollen grain concentration, where only thick-walled pollen are preserved. This part is interpreted as (salt) marshes comparable to the modern Everglades in the SE of North America. Graminoids, mostly of the family Cyperaceae, dominate the wetlands above peat layers (Willard et al., 2001), similar to the lignite layer found at the base of the section. Because these marshes occasionally fall dry, either periodically or during single events, the soils get oxidized, which may explain the bad preservation of the palynological remains and the absence of the thin-walled Cyperaceae pollen. The high amount of fern spores and the distribution of *Quercus*, *Celtis* and *Alnus* also fit to this modern equivalent. Tree islands with these taxa are frequently formed between the marshes (Willard et al., 2001; Denk et al., 2001).

Upsection, the fluvial influence is increasing, indicated by the contribution of hinterland taxa such as *Alnus*, *Symplocos*, *Carya*, Poaceae and especially Taxodiaceae (SPK-C1 −1 to 5). The trend climaxes in sample SPK-C1 5 (cluster IV) where Taxodiaceae are predominant and formed swamps (Fig. 7). This vegetation led to the formation of the second lignite layer. Clear freshwater conditions are further verified by the occurrence of freshwater gastropods, which shows that, at this time, the marine influenced part of estuary had retreated towards the basin. The establishment of large Taxodiaceae swamps can be a relatively rapid process, comparable to the modern Everglades, which formed in less than 5000 years (Gleason and Stone, 1994).

Afterwards, the environmental conditions quickly shift back to brackish and marine environments as obvious from the mollusc fauna. Consequently, the palynosamples show a constant increase of dinoflagellate cysts, dominated by the genus *Spiniferites* sp., which is a neritic element of eutrophic environments (Harland, 1983; Turon, 1994; Zonneveld, 1995). Along with the dinoflagellates, the green alga *Prasinophyta* is an important brackish water indicator and points towards rich nutrient content within the surface water. Today, *Prasinophyta* blooms are known from the Black Sea after heavy rainfall, which cause a decrease of the salinity of coastal waters and lead to eutrophic conditions (Vershinin, 2007).

During this interval (clusters II and III), the pollen assemblage clearly reflects the surrounding and hinterland vegetation. Typical plants dwelling next to salt water drained soils surrounding the shores of estuaries are Cyperaceae, Poaceae and Chenopodiaceae (Grigore and Toma, 2007; Jiang and Ding, 2008; González and Dupont, 2009). Alongside the tributaries and ponds within the wetlands, *Sparganium* and *Typha* were distributed (Britten and Crivelli, 1993), probably associated with the Lythraceae *Decodon*. This genus is common in the Miocene and has also been detected in the close-by locality Teiritzberg by SEM analysis (Kvaček and Sakala, 1999; Hofmann et al., 2002). The swamp vegetation is still represented by

Please cite this article as: Kern, A., et al., Millennial-scale vegetation dynamics in an estuary at the onset of the Miocene Climate Optimum, Palaeogeography, Palaeoclimatology, Palaeoecology (2010), doi:10.1016/j.palaeo.2010.07.014

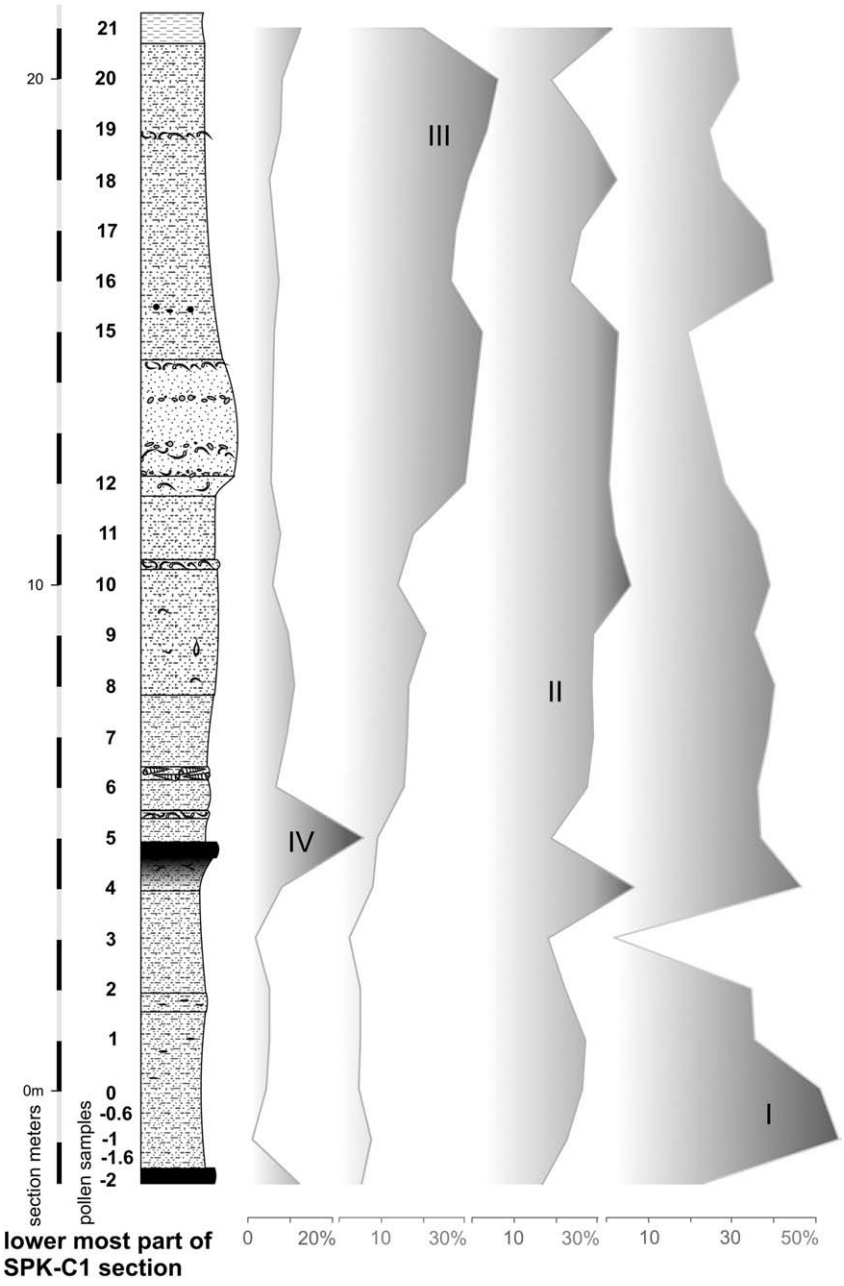

Fig. 7. The abundance of pollen and spore taxa, grouped according to the clusters shown in Fig. 6 (lithological details are given in Fig. 2B).

Taxodiaceae, such as *Taxodium* and *Glyptostrobus*, along with *Nyssa*, Tiliaceae and *Craigia* (Kvaček, 2003). These wetlands were sometimes overgrown by Pteridaceae, Arecaceae, and Apiaceae, but also trees like Arecaceae *Alnus*, *Fraxinus* or Oleaceae were inhabitants of this environment (cf. Utescher et al., 2009).

Some distance along the tributaries, riparian vegetation with abundant angiosperms developed. *Engelhardia*, *Carya* and *Pterocarya* are found along with other riparian plants such as *Salix*, *Fraxinus*, *Liquidambar* and the Ulmaceae *Ulmus* and *Zelkova* because of their ability to tolerate longer phases of inundation as are typical in such wetlands (Britten and Crivelli, 1993; Wilen and Tiner, 1993; Denk et al., 2001). The rest of the palyno-assemblages indicates forests with some open habitats in between, where Poaceae, other grasses and herbs were growing. A "Younger Mastixioid Flora" sensu Mai (1964) was developed including a high amount of broad-leaved evergreen and thermophilous elements. *Quercus* and *Fagus* were growing associated with Euphorbiaceae, Rutaceae, Sapotaceae and *Symplocos* (Jarvis and Clay-Poole, 1992). At somewhat higher elevations, *Abies* and *Picea* were common (cf. Jiménez-Moreno et al., 2008). Such low mountainous areas might have been formed by the Flysch-sandstone ridges bordering the Korneuburg Basin or by the young Alps in the south-west. The changing sea-level during the marine ingression caused slight alternations in the lateral distributions of these plant assemblages, but no taxon is dominating or disappearing within this part of the section.

At the top, the marine influence decreases again and dinoflagellates and Pinaceae pollen are replaced by angiosperms again. Additionally, especially Taxodiaceae pollen become more frequent again, indicating the re-establishment of swamp environments, due to the retreat of the sea from this part of the estuary.

Please cite this article as: Kern, A., et al., Millennial-scale vegetation dynamics in an estuary at the onset of the Miocene Climate Optimum, Palaeogeography, Palaeoclimatology, Palaeoecology (2010), doi:10.1016/j.palaeo.2010.07.014

5.2. Palaeoclimate

During the middle Burdigalian (regional Ottnangian and early Karpatian ages) the tropical Early Miocene climate of central Europe experienced a first cooling phase in the Miocene. This is recorded in the marine sphere by a distinct turnover of the mollusc fauna and a switch in the carbonate sedimentation towards a temperate bryomol facies (Harzhauser and Piller, 2007; Piller et al., 2007). Simultaneously, the frequency of tropical plant taxa declines and several tropical elements such as Sapotaceae disappear for a period of time (Planderová, 1990). Soon after, during the late Burdigalian (late Karpatian), the climate switched back towards subtropical conditions. Thermophilic molluscs display a distinct northward extension of their distribution area and Tethyan molluscs appear in the Paratethys Sea (Harzhauser et al., 2003; Harzhauser and Piller, 2007). In the terrestrial record, this warm phase is documented by the high number of thermophilic elements such as *Engelhardia*, *Platycarya*, Myricaceae and certain Fagaceae, Fabaceae and ferns (Doláková and Slamková, 2003). This trend indicates the onset of the Middle Miocene Climatic Optimum (MMCO) (Jiménez-Moreno et al., 2005).

The herein studied section represents a short, c. 21 kyr spanning interval of that early phase of the MMCO. Consequently, thermophile taxa such as *Engelhardia* and *Platycarya* are present in all samples and *Engelhardia* is even the most frequent angiosperm at all. Especially the abundant occurrence of *Engelhardia*, together with Mastixiaceae and Sapotaceae, points towards a warm and frost-free climate. Rutaceae, Areaceae, *Osmunda*, Schizaeaceae and *Ilex* are irregularly present, Rubiaceae and Araliaceae only sporadic, but their nearest living relatives today live all in tropical to subtropical climates. *Nyssa* and *Lonicera* indicate also a warm and mild climate (Fauquette et al., 2006; Kovar-Eder et al., 2006).

First climatic interpretations for the late Burdigalian of the Korneuburg Basin have already been performed based on various proxies: thermophilic ectothermic vertebrates suggest a humid subtropical climate with a minimum value of the mean annual temperature (MAT) of 17 °C, and the minimum cold month temperature (minCMT) ranging from at least 3 °C to about 8 °C (Böhme, 2003). The mean annual precipitation was estimated to range around 2000 mm (Meller, 1998). The marine gastropod fauna indicates minimum sea surface temperature values around 14—15 °C (Harzhauser et al., 2002). This estimate was supported by $\delta^{18}O$ studies, which document a range from 14 °C to 25 °C in coastal marine waters (Latal et al., 2005).

These estimates can now be tested and refined based on the palyno-assemblages. Herein we use the Coexistence Approach of Mosbrugger and Utescher (1997) which allows several palaeoclimate benchmarks such as the mean annual temperature (MAT), the mean temperature of the coldest and warmest months (CMT, WMT), the mean annual precipitation (MAP), the mean precipitation of the wettest and driest months (MPwet, MPdry) and the mean precipitation of the warmest month (MPwarm) to be estimated. Results of

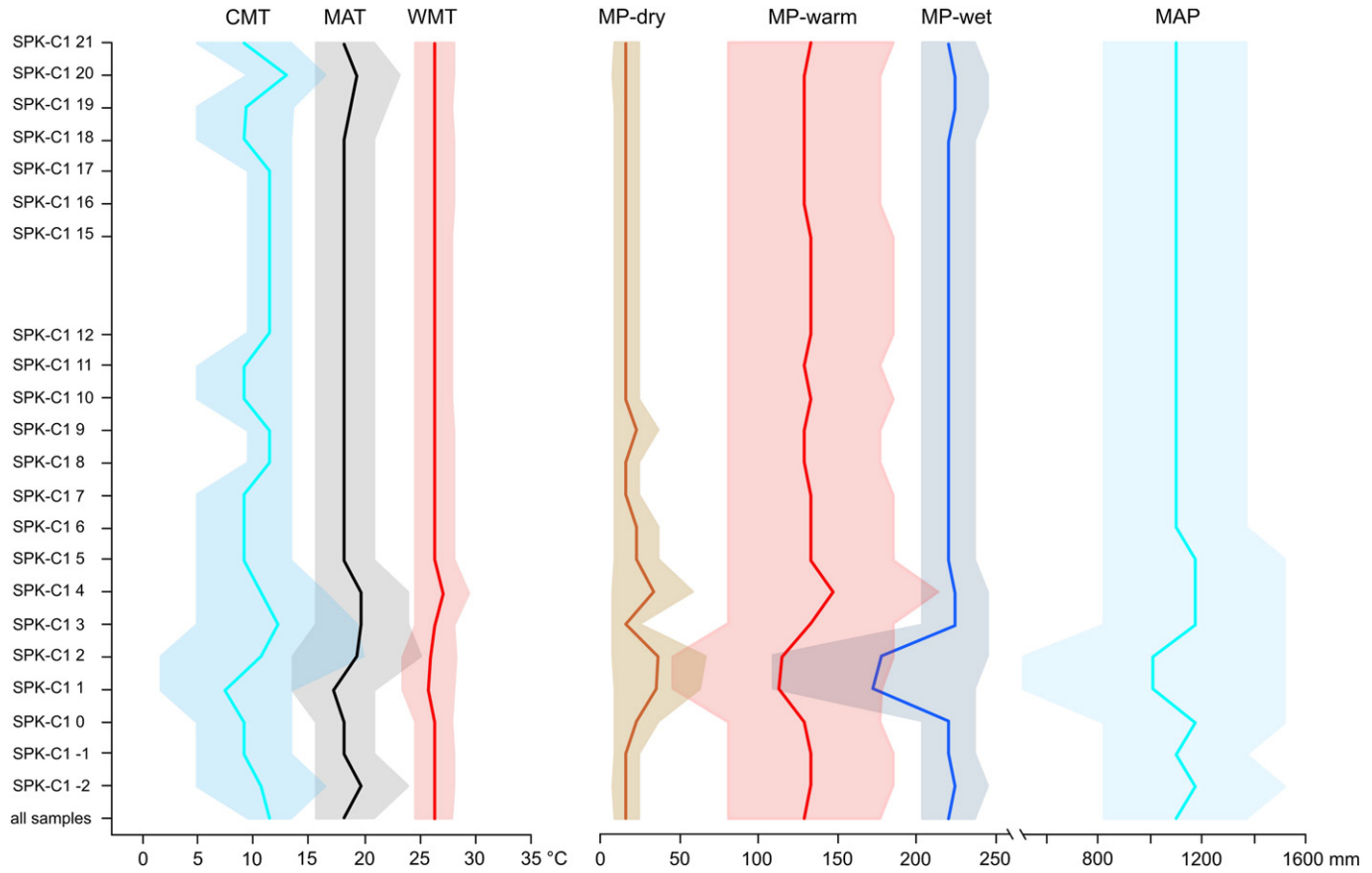

Fig. 8. Climate signals revealed by the Coexistence Approach of Mosbrugger and Utescher (1997). Shaded areas indicate the total range; middle line represents average values. The data suggest rather stable climatic conditions during the c. 21-kyr-interval. Nevertheless, shifts within the ranges would be unresolved due to the method used. Abbreviations: CMT: coldest month temperature, WMT: warmest month temperature, MAT: mean annual temperature, MAP: mean annual precipitation, MPwet, MPdry MPwarm: precipitation of the wettest, driest and warmest month.

Please cite this article as: Kern, A., et al., Millennial-scale vegetation dynamics in an estuary at the onset of the Miocene Climate Optimum, Palaeogeography, Palaeoclimatology, Palaeoecology (2010), doi:10.1016/j.palaeo.2010.07.014

the entire data set indicate a MAT of 15.7–20.8 °C, a CMT of 9.6–13.3 °C, and a WMT of 24.7–27.9 °C. Precipitation data comprise a MAP of 823–1372 mm, a MPwet of 204–236 mm, a MPdry of 9–24 mm and a MPwarm of 79–172 mm. This describes a much warmer and wetter climate that can be found today in this area (climatic data of Vienna). Each season is definitely colder, resulting in a MAT of 9.8 °C and a MAP of 660 mm. The colder season clearly shows frosts by a CMT of −1.4 °C but a higher rainfall of 39 mm. In contrast the warm season is colder (WMT: 19.9 °C), too, but also dryer (MPwarm: 84 mm) (Müller, 1996).

The temperature estimates based on the Coexistence Approach indicate a warm subtropical climate. A clear improvement to existing data is the evaluation of the coldest month temperature with c. 10 °C. This lower boundary is mostly defined by the common occurrence of *Mastixia* sp. The second important improvement is the rather low MAP which is about half of previous estimates. Moreover, a completely new and surprising aspect is the clear evidence of seasonality in these data. Up to now, the onset of the MMCO was assumed to correlate with an overall wet subtropical climate without marked seasonality (Kovar-Eder et al., 1998; Meller et al., 1999).

Our data, calculated with the Coexistence Approach and the Nearest Living Relatives concept, suggest that during the late Burdigalian, there was a wet season with a precipitation of 200 to 240 mm per month. In respect to the high precipitation results of the warmest month, it is likely that this wet season was the summer season. *Engelhardia*, *Symplocos* and Taxodiaceae occur today in similar climates with clear seasonality. Especially the mixture of *Symplocos*, together with *Betula* and *Quercus*, points to the existence of a warm and wet season. This was contrasted by a quite dry season, lasting at least one month, with a rainfall of less than 30 mm (Fig. 8), which is suggested mostly by the occurrence of *Celtis*, *Sparganium* and the subtropical taxon *Platycarya*.

Comparable climate parameters were proposed for the more continental late Burdigalian settings in southern and north-western Germany by Böhme et al. (2007) and Utescher et al. (2000). Therefore, this climate pattern with dry and slightly cooler winter seasons and humid and warm summer seasons seems to have characterized Central Europe at the onset of the MMCO. These data suggest similarities with the modern Cwa climate of Koeppen (1936). Today this climate covers parts of northern India extending into south-eastern Asia (south Nepal, Myanmar, northern Thailand) to East China and in central south Africa (east Angola, Zambia, north Zimbabwe, north Mozambique) (Peel et al., 2007).

5.3. The pace of environmental change

Although the suggested 21-kyr-precessional cyclicity is supported by power spectra analysis of the entire SPK-C + SPK-C1 sections, the conversion into a time model for the investigated part of the SPK-C1 section is difficult. Sedimentation will not have been completely constant throughout the interval. In-situ occurrences of *Turritella* coquinas and of bivalves in life-position are good indicators for undisturbed sedimentation in large parts of the section. In contrast, pebble lags and tempestitic coquinas in the sand layers at 12–14 m point to winnowing and re-sedimentation. Despite these uncertainties, the conversion of the average sedimentation rate of 800–1100 cm per ky into a time model will allow a rough estimation of the pace of environmental change.

Hence, the basal formation of salt marshes and peat bogs characterized the locality for about 5000–6000 years. As in the modern Everglades, these environments graded into Taxodiaceae swamps which seem to have developed very quickly within less than 2000 years. The subsequent marine ingression was not a gradual process but rather a very swift take-over. The swamps drowned within a few decades and made way for lagoonal marine mollusc assemblages. The transgressive pulse culminated within c. 8000 years in the establishment of highly dynamic shore and foreshore environments. Within another 5000–7000 years, the fully marine conditions switched gradually back and a progradation of swampy conditions took place.

Despite the very clear cyclicity in the sedimentary record, the analysis of the palaeo-vegetation provides no hint of major cyclic climate changes. Therefore, we suggest that the rhythm in the sea-level record was not coupled with a climatic cyclicity in the investigation area. This result, however, may also be an artifact, if the amplitudes of the climatic parameters are too low to be resolved by the Coexistence Approach. On the other hand, the factors influencing the relative sea-level of the huge early Miocene Eurasian Paratethys may not be expressed in the investigation area, which was only a minor appendix.

6. Conclusions

The onset of the Middle Miocene Climate Optimum during the late Burdigalian in Central Europe coincided with considerable seasonality. A warm and wet summer season with a precipitation of 204–236 mm during the wettest month was opposed by a rather dry winter season with very low precipitation of c. 9–24 mm in the driest month and temperatures which did not drop significantly below 10 °C. The vegetational dynamics in this late Early Miocene estuary were rapid. Major marine ingressions which drowned the marshes and swamps happened within few decades or centuries. The establishment of Taxodiaceae swamps was a rapid process as well which took few millennia. Only the regression of the sea and the coinciding progradation of estuarine and wetland settings was a gradual progress.

The assumption that the statistically significant sedimentary rhythm of the section is related to the 21-kyr-precession cycle is supported by several Middle Miocene wells in the Vienna Basin which document a clear reflection of the precessional and eccentricity cycles (Hohenegger et al., 2008; Lirer et al., 2009). Despite the clear cyclicity in the sedimentary record, however, the palyno-spectra reflect rather stable climatic conditions during the investigated interval (Fig. 8). Quantitative changes in the composition of the palyno-assemblages, as obvious in the cluster analysis, seem to be triggered only by shifting local environments bound to periodic marine ingressions into the wetlands of the Korneuburg Basin. This in turn, suggests that the – probably astronomically forced – cyclicity of the sea-level was not coupled with a climatic cyclicity in the investigation area. This misfit might be explained by the fact that the Central Paratethys was just an appendix of the Western Tethys Ocean during the late Burdigalian (Rögl, 1998). Therefore, the mechanisms forcing the hydrological budget of the huge Western Tethys Ocean are not necessarily visible in its northern embayment on a regional scale. A second explanation might be that the climatic amplitude is below the methodological resolution of the Coexistence Approach due to the broad climatic range of c. 5 °C for the MAT and of c. 500 mm for the MAP of the subtropical vegetation of the Korneuburg Basin.

Acknowledgements

The study was supported by the FWF-grants P21414-B16 (Millennial- to centennial-scale vegetation dynamics and surface water productivity during the Late Miocene in and around Lake Pannon) and the Geological Survey of Austria. It contributes to the NECLIME network.

Many thanks to Andreas Kroh (NHM) for identifications of the starfish remains.

Please cite this article as: Kern, A., et al., Millennial-scale vegetation dynamics in an estuary at the onset of the Miocene Climate Optimum, Palaeogeography, Palaeoclimatology, Palaeoecology (2010), doi:10.1016/j.palaeo.2010.07.014

Appendix A

The appendix lists all by the Coexistence Approach reconstructed climatic intervals for each sample including the number of taxa contributing to create this data and the taxa, which were excluded.

Coexistence Approach data.

All samples	MAT	15.7	20.8	CMT	9.6	13.3	WMT	24.7	27.9	MAP	823	1372	MPwet	204	236	MPdry	9	24	MPwarm	79	172
	Number of analysed taxa				36		Excluded taxa			*Catahya*, *Sciadopitys*										
SPK-C1 −2.0	MAT	15.6	23.9	CMT	5.0	16.4	WMT	24.7	28.1	MAP	823	1520	MPwet	204	245	MPdry	8	24	MPwarm	79	180
	Number of analysed taxa				14		Excluded taxa			*Picea*, *Catahya*										
SPK-C1 −1.6	MAT	15.6	21.9	CMT	5.0	13.6	WMT	24.7	28.1	MAP	823	1520	MPwet	204	245	MPdry	8	59	MPwarm	79	180
	Number of analysed taxa				13		Excluded taxa			*Cathaya*										
SPK-C1 −1.0	MAT	15.6	20.8	CMT	5.0	13.3	WMT	24.7	28.1	MAP	823	1372	MPwet	204	236	MPdry	9	24	MPwarm	79	180
	Number of analysed taxa				13		Excluded taxa			*Cathaya*										
SPK-C1 −0.6	MAT	15.6	20.8	CMT	5.0	13.3	WMT	24.7	28.1	MAP	823	1520	MPwet	204	236	MPdry	9	24	MPwarm	82	172
	Number of analysed taxa				16		Excluded taxa			*Cathaya*, *Sciadopitys*										
SPK-C1 0.0	MAT	15.6	20.8	CMT	5.0	13.3	WMT	24.7	27.9	MAP	823	1520	MPwet	204	236	MPdry	9	37	MPwarm	79	172
	Number of analysed taxa				19		Excluded taxa			*Catahya*										
SPK-C1 1.0	MAT	13.6	20.8	CMT	1.8	13.3	WMT	23.6	28.1	MAP	505	1520	MPwet	109	236	MPdry	9	64	MPwarm	45	180
	Number of analysed taxa				10		Excluded taxa			*Ephedra*, *Catahya*										
SPK-C1 2.0	MAT	13.6	25.0	CMT	1.8	19.8	WMT	23.6	28.3	MAP	505	1520	MPwet	109	245	MPdry	8	67	MPwarm	45	180
	Number of analysed taxa				5		Excluded taxa			*Picea*, *Catahya*										
SPK-C1 3.0	MAT	15.6	23.9	CMT	5.0	19.4	WMT	24.7	28.1	MAP	823	1520	MPwet	204	245	MPdry	8	24	MPwarm	79	180
	Number of analysed taxa				8		Excluded taxa			*Picea*, *Catahya*										
SPK-C1 4.0	MAT	15.6	23.9	CMT	5.0	16.4	WMT	24.7	29.5	MAP	823	1520	MPwet	204	245	MPdry	8	59	MPwarm	79	208
	Number of analysed taxa				6		Excluded taxa			*Catahya*										
SPK-C1 5.0	MAT	15.6	20.8	CMT	5.0	13.3	WMT	24.7	28.1	MAP	823	1520	MPwet	204	236	MPdry	9	37	MPwarm	79	180
	Number of analysed taxa				15		Excluded taxa			*Catahya*										
SPK-C1 6.0	MAT	15.6	20.8	CMT	5.0	13.3	WMT	24.7	28.1	MAP	823	1372	MPwet	204	236	MPdry	9	37	MPwarm	79	180
	Number of analysed taxa				22		Excluded taxa			*Catahya*										
SPK-C1 7.0	MAT	15.6	20.8	CMT	5.0	13.3	WMT	24.7	28.1	MAP	823	1372	MPwet	204	236	MPdry	9	24	MPwarm	79	180
	Number of analysed taxa				25		Excluded taxa			*Catahya*										
SPK-C1 8.0	MAT	15.7	20.8	CMT	9.6	13.3	WMT	24.7	28.1	MAP	823	1372	MPwet	204	236	MPdry	9	24	MPwarm	79	172
	Number of analysed taxa				26		Excluded taxa			*Catahya*, *Sciadopitys*										
SPK-C1 9.0	MAT	15.7	20.8	CMT	9.6	13.3	WMT	24.7	28.1	MAP	823	1372	MPwet	204	236	MPdry	9	37	MPwarm	79	172
	Number of analysed taxa				21		Excluded taxa			*Catahya*										
SPK-C1 10.0	MAT	15.6	20.8	CMT	5.0	13.3	WMT	24.7	27.9	MAP	823	1372	MPwet	204	236	MPdry	9	24	MPwarm	79	180
	Number of analysed taxa				22		Excluded taxa			*Catahya*, *Sciadopitys*										
SPK-C1 11.0	MAT	15.6	20.8	CMT	5.0	13.3	WMT	24.7	27.9	MAP	823	1372	MPwet	204	236	MPdry	9	24	MPwarm	79	172
	Number of analysed taxa				24		Excluded taxa			*Ephedra*, *Catahya*										
SPK-C1 12.0	MAT	15.7	20.8	CMT	9.6	13.3	WMT	24.7	27.9	MAP	823	1372	MPwet	204	236	MPdry	9	24	MPwarm	79	180
	Number of analysed taxa				25		Excluded taxa			*Ephedra*, *Catahya*										
SPK-C1 13.0	MAT	0.0	0.0	CMT	0.0	0.0	WMT	0.0	0.0	MAP	0	0	MPwet	0	0	MPdry	0	0	MPwarm	0	0
	Number of analysed taxa				0		Excluded taxa			None										
SPK-C1 14.0	MAT	0.0	0.0	CMT	0.0	0.0	WMT	0.0	0.0	MAP	0	0	MPwet	0	0	MPdry	0	0	MPwarm	0	0
	Number of analysed taxa				0		Excluded taxa			None										
SPK-C1 15.0	MAT	15.7	20.8	CMT	9.6	13.3	WMT	24.7	27.9	MAP	823	1372	MPwet	204	236	MPdry	9	24	MPwarm	79	180
	Number of analysed taxa				25		Excluded taxa			*Catahya*										
SPK-C1 16.0	MAT	15.7	20.8	CMT	9.6	13.3	WMT	24.7	28.1	MAP	823	1372	MPwet	204	236	MPdry	9	24	MPwarm	79	172
	Number of analysed taxa				21		Excluded taxa			*Catahya*, *Sciadopitys*										
SPK-C1 17.0	MAT	15.7	20.8	CMT	9.6	13.3	WMT	24.7	28.1	MAP	823	1372	MPwet	204	236	MPdry	9	24	MPwarm	79	172
	Number of analysed taxa				28		Excluded taxa			*Catahya*										
SPK-C1 18.0	MAT	15.6	20.8	CMT	5.0	13.3	WMT	24.7	28.1	MAP	823	1372	MPwet	204	236	MPdry	9	24	MPwarm	79	172
	Number of analysed taxa				24		Excluded taxa			*Catahya*, *Sciadopitys*										
SPK-C1 19.0	MAT	15.6	21.9	CMT	5.0	13.6	WMT	24.7	27.9	MAP	823	1372	MPwet	204	245	MPdry	9	24	MPwarm	79	172
	Number of analysed taxa				22		Excluded taxa			*Picea*, *Catahya*, *Sciadopitys*										
SPK-C1 20.0	MAT	15.7	23.1	CMT	9.6	16.4	WMT	24.7	28.1	MAP	823	1372	MPwet	204	245	MPdry	8	24	MPwarm	79	172
	Number of analysed taxa				19		Excluded taxa			*Catahya*, *Sciadopitys*										
SPK-C1 21.0	MAT	15.6	20.8	CMT	5.0	13.3	WMT	24.7	28.1	MAP	823	1372	MPwet	204	236	MPdry	9	24	MPwarm	79	180
	Number of analysed taxa				24		Excluded taxa			*Picea*, *Catahya*, *Sciadopitys*										

Abbreviations: CMT: coldest month temperature, WMT: warmest month temperature, MAT: mean annual temperature, MAP: mean annual precipitation, MPwet, MPdry MPwarm: precipitation of the wettest, driest and warmest months.
Temperature data is given in °C, precipitation in mm per year/per month.

References

Baldi, T., 1973. Mollusc Fauna of the Hungarian Upper Oligocene (Egerian). Akadémiai Kiado, Budapest.

Behling, H., Cohen, M.C.L., Lara, R.J., 2001. Studies on Holocene mangrove ecosystem dynamics of the Bragança Peninsula in north-eastern Pará, Brazil. Palaeogeography, Palaeoclimatology, Palaeoecology 167, 225–242.

Böhme, M., 2003. Miocene Climatic Optimum: evidence from lower vertebrates. Palaeogeography, Palaeoclimatology, Palaeoecology 195, 389–401.

Böhme, M., Bruch, A., Selmeier, A., 2007. The reconstruction of Early and Middle Miocene climate and vegetation in Southern Germany as determined from the fossil wood flora. Palaeogeography, Palaeoclimatology, Palaeoecology 253, 91–114.

Britten, R.H., Crivelli, A.J., 1993. Wetlands of southern Europe and North Africa: Mediterranean wetlands. In: Whigham, D.F., Dykyjová, D., Hejný, S. (Eds.), Handbook of Vegetation Science, Wetlands of the World I: Inventory, Ecology and Management. Kluver Academic Publishers, Dordrecht, pp. 129–194.

Daxner-Höck, G., 1998. Säugetiere (Mammalia) aus dem Karpat des Korneuburger Beckens. 3. Rodentia und Carnivora. Beiträge zur Paläontologie 23, 367–408.

Please cite this article as: Kern, A., et al., Millennial-scale vegetation dynamics in an estuary at the onset of the Miocene Climate Optimum, Palaeogeography, Palaeoclimatology, Palaeoecology (2010), doi:10.1016/j.palaeo.2010.07.014

Debenay, J.-P., Pages, J., Guillou, J.-J., 1994. Transformation of a subtropical river into a hyperhaline estuary: the Casamance River (Senegal) — paleogeographical implications. Palaeogeography, Palaeoclimatology, Palaeoecology 107, 103–119.

Denk, T., Frotzler, N., Davitashvili, N., 2001. Vegetational patterns and distribution of relict taxa in humid temperate forests and wetlands of Georgia (Transcaucasia). Biologocal Journal of the Linnean Sociaty 72, 287–332.

Doláková, N., Slamková, M., 2003. Palynological characteristics of Karpatian sediments. In: Brzobohatý, R., Cicha, I., Kovác, M., Rögl, F. (Eds.), The Karpatian — a Lower Miocene Stage of the Central Paratethys. Masaryk University, Brno, pp. 325–345.

Donoghue, J.F., 1989. Trends in Chesapeake Bay sedimentation rates during the late Holocene. Quaternary Research 34, 33–46.

Ellison, J., 2005. Holocene palynology and sea-level change in two estuaries in Southern Irian Jaya. Palaeogeography, Palaeoclimatology, Palaeoecology 220, 291–309.

Erdtman, G., 1954. An Introduction to Pollen Analysis. Chronica Botanica Company, Waltham, Massachusetts.

Fauquette, S., Suc, J.-P., Bertini, A., Popescu, S.-M., Warny, S., Bachiri Taoufiq, N., Perez Villa, M.-J., Chikhi, H., Feddi, N., Subally, D., Clauzon, G., Ferrier, J., 2006. How much did climate forace the Messinian salinity crisis? Quantified climatic conditions from pollen recods in the Mediterranean region. Palaeogeography, Palaeoclimatology, Palaeoecology 238, 281–301.

Gleason, P.J., Stone, P., 1994. Age, origin, and landscape evolution of the Everglades peatland. In: Davis, S.M., Ogden, J.C. (Eds.), Everglades: The Ecosystem and its Restauration. St. Lucie Press, Delray, Florida, pp. 149–197.

González, C., Dupont, L.M., 2009. Tropical salt marsh succession as sea-level indicator during Heinrich events. Quaternary Science Reviews 28, 939–946.

Gribben, P.E., Helson, J., Millar, R., 2004. Population abundance estimates of the New Zealand geoduck clam, *Panopea zelandica*, using North American methodology: is the technology transferable? Journal of Shellfish Research 23, 683–691.

Grigore, M.N., Toma, C., 2007. Histo-anatomical strategies of Chenopodiaceae halophytes: adaptive, ecological and evolutionary implications. WSEAS Transaction on Biology and Biomedcine 12 (4), 204–218.

Grimm, E.C., 2004. Tilia and TG View Version 2.0.2. Illinois State Museum, Research and Collector Center.

Hammer, Ø., Harper, D.A.T., Ryan, P.D., 2001. PAST; palaeontological statistics software package for education and data analysis. Palaeontologica Electronica 4 (1), 9.

Harland, R., 1983. Distribution map of recent Dionflagellate cysts in bottom sediments from the North Atlantic Ocean and adjaceted seas. Palaeontology 26, 321–387.

Harzhauser, M., Mandic, O., 2002. Late Oligocene Gastropods and Bivalves from the Lower and Upper Austrian Molasse Basin. In: Piller, W.E., Rasser, M. (Eds.), The Paleogene of Austria. Österreichische Akademie der Wissenschaften, Schriftenreihe der Erdwissenschaftlichen Kommission 14, Vienna, pp. 671–795.

Harzhauser, M., Piller, W.E., 2007. Benchmark data of a changing sea — palaeogeography, plaeobiogeography and events in the Central Paratethys during the Miocene. Palaeogeography, Palaeoclimatology, Palaeoecology 253, 8–31.

Harzhauser, M., Böhme, M., Mandic, O., Hofmann, Ch.-C.h., 2002. The Karpatian (Late Burdigalian) of the Korneuburg Basin — a palaeoecological and biostratigraphical synthesis. Beiträge zur Paläontologie 27, 441–456.

Harzhauser, M., Mandic, O., Zuschin, M., 2003. Changes in Paratethyan marine molluscs at the Early/Middle Miocene transition — diversity, paleogeography and paleoclimate. Acta Geologica Polonica 53, 323–339.

Harzhauser, M., Sovis, W., Kroh, A., 2009. Das verschwundene Meer. Naturhistorisches Museum, Wien978-3-902421-42-5.

Hendler, G., Miller, J.E., Pawson, D.E., Kier, P.M., 1995. Sea Stars, Sea Urchins, and Allies. Smithsonian Institution Press, Washington, DC.

Hofmann, Ch.-C.h., Zetter, R., Draxler, I., 2002. Pollen- und Sporenvergesellschaftungen aus dem Kapatium des Korneuburger Beckens (Niederosterreich). Beiträge zur Paläontologie 27, 17–43.

Hohenegger, J., Coric, S., Khatun, M., Pervesler, P., Rögl, F., Rupp, C., Selge, A., Uchman, A., Wagreich, M., 2008. Cyclostratigraphic dating in the Lower Badenian (Middle Miocene) of the Vienna Basin (Austria): the Baden-Sooss core. International Journal of Earth Sciences 98, 915–930.

Jarvis, D.I., Clay-Poole, S.T., 1992. A comparison of modern pollen rain and vegetation in southwestern Sichuan Province, China. Review of Palaeobotany and Palynology 75, 239–258.

Jiang, H., Ding, Z., 2008. A 20 Ma pollen record of East-Asian summer monsoon evolution from Guyuan, Ningxia, China. Palaeogeography, Palaeoclimatology, Palaeoecology 265, 30–38.

Jiménez-Moreno, G., Rodríguez-Tovar, F.I., Pardo-Igúzquiza, E., Fauquette, S., Suc, J.P., Müller, P., 2005. High-resolution palynological analysis in the late early-middle Miocene core from the Pannonian Basin, Hungary: climatic changes, astronimical forcing and eustatic fluctuations in the Central Paratethys. Palaeogeography, Palaeoclimatology, Palaeoecology 216, 73–97.

Jiménez-Moreno, G., Fauquette, S., Suc, J.-P., 2008. Vegetation, climate and palaeoaltitude reconstructions of the Eastern Alps during the Miocene based on pollen records from Austria, Central Europe. Journal of Biogeography 35, 1638–1649.

Kamaruzzaman, B.Y., Ong, M.C., 2008. Recent sedimentation rate and sediment ages determination of Kemaman-Chukai Mangrove Forest, Terengganu, Malaysia. American Journal of Agricultural and Biological Sciences 3, 522–525.

Klaus, W., 1987. Einführung in die Paläobotanik. Band I. Franz Deuticke Verlagsgesellschaft, Vienna.

Koeppen, W., 1936. Das geographische System der Klimate. In: Koeppen, W., Geiger, R. (Eds.), Handbuch der Klimatologie. Bebrüder Bornträger, Berlin, pp. 1–44.

Kovar-Eder, J., Meller, B., Zetter, R., 1998. Comparative investigations on the basal fossiliferous layers at the opencast mine Oberndorf (Köflach-Voitsberg lignite deposits, Styria, Austria; Early Miocene). Review of Palaeobotany and Palynology 101, 125–145.

Kovar-Eder, J., Kvaček, Z., Martinetto, E., Roiron, P., 2006. Late Miocene to Early Pliocene vegetation of southern Europe (7–4 Ma) as reflected in the megafossil plant record. Palaeogeography, Palaeoclimatology, Palaeoecology 238, 321–339.

Kvaček, Z., 2003. The flora and vegetation of the Karpatian. In: Brzobohatý, R., Cicha, I., Kovác, M., Rögl, F. (Eds.), The Karpatian — a Lower Miocene Stage of the Central Paratethys. Masaryk University, Brno, pp. 347–351.

Kvaček, Z., Sakala, J., 1999. Twig with attached leaves, fruits and seeds of Decodon (Lythraceae) from the Lower Miocene of northern Bohemia, and implications for the identification of detached leaves and seeds. Review of Palaeobotany and Palynology 107, 201–222.

Latal, C., Piller, W.E., Harzhauser, M., 2005. Small-scaled environmental changes: indications from stable isotopes of gastropods (Early Miocene, Korneuburg Basin, Austria). International Journal of Earth Sciences 95, 95–106.

Li, Z., Saito, Y., Matsumoto, E., Wang, Y., Haruyama, S., Hori, K., Doanh, L.Q., 2006. Palynological record of climate change during the last deglaciation from the Song Hong (Red River) delta, Vietnam. Palaeogeography, Palaeoclimatology, Palaeoecology 235, 406–430.

Lirer, F., Harzhauser, M., Pelosi, N., Piller, W.E., Schmid, H.P., Sprovieri, M., 2009. Astronomically forced teleconnection between Paratethyan and Mediterrean sediments during the Middle and Late Miocene. Palaeogeography, Palaeoclimatology, Palaeoecology 275, 1–13.

Lynch, J.C., Meriwether, J.R., McKee, B.A., Vera-Herrera, F., Twinlley, R.R., 1989. Recent accretion in mangrove ecosystems based on ^{137}Cs and ^{210}Pb. Estuaries 4, 284–299.

Mai, D.H., 1964. Die Mastixioideen-Floren im Tertiär der Oberlausitz. Paläontologische Abhandlungen B 2, 1–192.

Mandic, O., Harzhauser, M., Schlaf, J., Piller, W.E., Schuster, F., Wielandt-Schuster, U., Nebelsick, J.H., Kroh, A., Rögl, F., Bassant, P., 2004. Palaeoenvironmental reconstruction of an epicontinental flooding — Burdigalian (Early Miocene) of the Mut Basin (Southern Turkey). Courier Forschungsinstitut Senckenberg 248, 57–92.

Mandic, O., Harzhauser, M., Roetzel, R., Tibuleac, P., 2008. Benthic mass-mortality events on a Middle Miocene incised-valley tidal-flat (North Alpine Foredeep Basin). Facies 54, 343–359.

Martini, E., 1971. Standard Tertiary and Quaternary calcareous nannoplankton zonation. In: Farinacci, A. (Ed.), Proceedings of the II. Planktonic Conference. Tecnoscienza, Roma, pp. 739–785.

Márton, E., 2008. Palaeomagnetism and paleogeography. In: Rasser, M. and Harzhauser, M. (Eds.), Palaeogene and Neogene. In.: McCann, T. (Ed.), The Geology of Central Europe, Volume 2: Mesozoic and Cenozoic. Geological Society, London, pp. 1033–1035.

Meller, B., 1998. Karpo-Taphocoenosen aus dem Karpat des Korneuburger Beckens (Unter-Miozän; Niederösterreich) — ein Beitrag zur Vegetationsrekonstruktion. Beiträge zur Paläontologie 23, 85–121.

Meller, B., Kovar-Eder, J., Zetter, R., 1999. Lower Miocene diaspore-, leaf- and palynomorph-assemblage from the base of the lignite-bearing sequence in the opencast mine Oberdorf N Voitsberg (Styria, Austira) as indication of a "Younger Mastixioid" vegetation. Palaeontographica Abt. B 252, 123–178.

Mosbrugger, V., Utescher, T., 1997. The Coexistence Approach — a new method for quantitative reconstructions of Teriary terrestrial paleoclimate data using plant fossils. Palaeogeoraphy, Palaeoclimatology, Palaeoecology 134, 61–86.

Müller, M.J., 1996. Handbuch ausgewählter Klimastationen der Erde. Forschungsstelle Bodenerosion Universität Trier, Mertesdorf (Ruwertal).

Patchineelam, S.R., Smoak, J.M., 1999. Sediment accumulation rates along the Inner Eastern Brazilian continental shelf. Geo-Marine Letters 19, 196–201.

Peel, M.C., Finlayson, B.L., McMahon, T.A., 2007. Updated world map of the Köppen-Geiger climate classification. Hydrology and Earth System Science Discussions 4, 439–473.

Piller, W.E., Harzhauser, M., Mandic, O., 2007. Miocene Central Paratethys stratigraphy — current status and future directions. Stratigraphy 4, 151–168.

Planderová, E., 1990. Miocene Microflora of Slovak Central Paratethys and its Biostratigraphical Significance. Dionýz Štúr Institute of Geology, Bratislava.

Rögl, F., 1998. Palaeogeographic considerations for Mediterranean and Paratethys Seaways (Oligocene to Miocene). Annalen des Naturhistorischen Museums in Wien 99, 279–310.

Scholger, R., 1998. Magnetostratigraphic and palaeomagnetic analysis from the Early Miocene (Karpatian) deposits Teiritzberg and Obergänserndorf (Korneuburg Basin, Lower Austria). Beiträge zur Paläontologie 23, 25–26.

Smoak, J.M., Patchineelam, S.R., 1999. Sediment mixing and accumulation in a mangrove ecosystem: evidence from ^{210}Pb, ^{234}Th and ^{7}Be. Mangroves and Salt Marshes 3, 17–27.

Sovis, W., Schmid, B., 1998. Das Karpat des Korneuburger Beckens, Teil 1. Beiträge zur Paläontologie 23, 1–413.

Sovis, W., Schmid, B., 2002. Das Karpat des Korneuburger Beckens, Teil 2. Beiträge zur Paläontologie 27, 1–467.

Turon, J., 1994. Le palynoplancton dans l'environment de l'Atlantique nord-oriental Évolution climatique et hydrologique depuis le dernier maximum glaciaire. Docorat ès sciences thesis, Université Bordeaux I, Mémoire de l'Institut de Géologie du Bassin d'Aquitaine.

Utescher, T., Mosbrugger, V., Ashraf, A.R., 2000. Terrestrial climate evolution in Northwest Germany over the last 25 million years. Palaios 15, 430–449.

Utescher, T., Ivanov, D., Harzhauser, M., Bozukov, V., Ashraf, A.R., Rolf, C., Urbat, M., Mosbrugger, V., 2009. Cyclic climate and vegetation change in the late Miocene of Western Bulgaria. Palaeogeography, Palaeoclimatology, Palaeoecology 272, 99–114.

Van Santen, P., Augustinus, P.G.E.F., Janssen-Stelder, B.M., Quartel, S., Tri, N.H., 2007. Journal of Asian Earth Sciences 29, 566–575.

Vershinin, A., 2007. Book Living Black Sea. Kogorta Publishers, Krasnodar- Moscow.

Please cite this article as: Kern, A., et al., Millennial-scale vegetation dynamics in an estuary at the onset of the Miocene Climate Optimum, Palaeogeography, Palaeoclimatology, Palaeoecology (2010), doi:10.1016/j.palaeo.2010.07.014

Wessely, G., 1998. Geologie des Korneuburger Beckens. Beiträge zur Paläontologie 23, 9–23.
Wilen, B.O., Tiner, R.W., 1993. Wetlands of the United States. In: Whigham, D.F., Dykyjová, D., Hejný, S. (Eds.), Handbook of Vegetation Science, Wetlands of the World I: Inventory, Ecology and Management. Kluwer Academic Publishers, Dordrecht, pp. 129–194.
Willard, D.A., Weimer, L.M., Riegel, W.L., 2001. Pollen assemblage as paleoenvironment proxies in the Florida Everglades. Review of Palaeobotany and Palynology 113, 213–253.
Zonneveld, K.A.F., 1995. Palaeoclimatic and palaeo-ecological changes during the last deglaciation in the Eastern Mediterranean — implications for dinoflagellates ecology. Review of Palaeobotany and Palynology 84, 221–253.
Zuschin, M., Harzhauser, M., Mandic, O., 2004. Palaeoecology and taphonomy of a single parautochthonous Paratethyan tidal flat deposit (Karpatian, Lower Miocene — Kleinebersdorf, Lower Austria). Courier Forschungsinstitut Senckenberg 246, 153–168.

Please cite this article as: Kern, A., et al., Millennial-scale vegetation dynamics in an estuary at the onset of the Miocene Climate Optimum, Palaeogeography, Palaeoclimatology, Palaeoecology (2010), doi:10.1016/j.palaeo.2010.07.014